

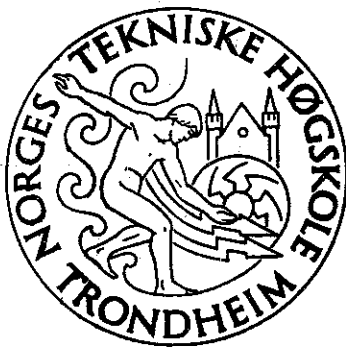
*Handwritten signature and date:*  
18/1/75

**A CRITICAL REVIEW OF  
THE HYDRAULICS OF RUBBLE MOUND STRUCTURES**

**FORCES BY UPRUSH AND DOWNRUSH  
THE IMPORTANCE OF PERMEABILITY  
THE RESONANCE PHENOMENON  
FRICTION BETWEEN ARMOR BLOCKS  
AND BETWEEN ARMOR AND SUBLAYER  
SLOPE GEOMETRY  
PRACTICAL DESIGN PRINCIPLES**

by

**Per Bruun and Palmi Johannesson**



**DIVISION OF PORT AND OCEAN ENGINEERING**

**THE UNIVERSITY OF TRONDHEIM**

**THE NORWEGIAN INSTITUTE OF TECHNOLOGY**

**TRONDHEIM, NORWAY**

A CRITICAL REVIEW OF THE  
HYDRAULICS OF RUBBLE MOUND STRUCTURES

INDEX

PART I

FORCES BY UPRUSH AND DOWNRUSH  
THE IMPORTANCE OF PERMEABILITY

INTRODUCTION	p. 1
REVIEW OF FORCES ON AN ARMOR UNIT PLACED IN A RUBBLE STRUCTURE	pp. 2 - 3
DETAILED DISCUSSION OF REASONS FOR FAILURE	pp. 3 - 20
UPRUSH AND DOWNRUSH	pp. 4 - 11
THE IMPORTANCE OF POROSITY (PERMEABILITY)	pp. 11 - 19
DISCUSSION AND CONCLUSION	
THE RESONANCE PHENOMENON	p. 20
REFERENCES	pp. 21 - 23

PART II

FRICTION BETWEEN ARMOR BLOCKS  
AND BETWEEN ARMOR AND SUBLAYER  
SLOPE GEOMETRY

INTRODUCTION	p. 24
FRICTION FORCES	pp. 24 - 32
SLOPE GEOMETRY	pp. 32 - 37
DISCUSSION, PART I AND II	pp. 37
PRACTICAL DESIGN PRINCIPLES	pp. 38 - 39
CONCLUSION, PART I AND II	pp. 39 - 43
REFERENCES	pp. 44
FIGURES	pp. 45 - 58
LIST OF PUBLICATIONS AND REPORTS BY THE DIV. OF PORTS AND OCEAN ENGINEERING 1970-1974	pp. 59 - 65

# NOTATION

$B$	Buoyancy
$D$	Diameter of sphere
$C_D$	Drag coefficient
$C_L$	Lift coefficient
$C_I$	Inertia force coefficient
$F_P$	Slope parallel force on object
$F_n$	Normal force on object on slope
$F_D$	Shear force on object
$F_I$	Inertia force on object
$F_L$	Lift force on object
$F_{core}$	Force from the core of the mound
$G$	Gravity force
$M$	Moment
$N$	Number (of blocks or spheres)
$T$	Contact pressure
$t$	Time
$U$	Water velocity
$V_P$	Velocity parallel to slope
$V_n$	Velocity normal to slope
$W$	Weight of block or sphere
$\rho_s$	Density of object
$\rho_w$	Density of water
$\mu, k$	Roughness parameters, defined in each particular case
$\alpha, \beta, \phi$	Angles, defined in each particular case

# A CRITICAL REVIEW OF THE HYDRAULICS OF RUBBLE MOUND STRUCTURES

## PART I

### FORCES BY UPRUSH AND DOWNRUSH THE IMPORTANCE OF PERMEABILITY

Per Bruun and Palmi Johannesson

#### INTRODUCTION

This paper is the result of several years of research at the Norwegian Institute of Technology. It comprises a critical review of the hydraulics of rubble mound structures including analyses of forces by uprush and downrush, forces occurring in the toe of a wave breaking on a slope, hydrostatic pressures due to permeability of the structure, friction forces between armor and sublayer(s) and forces between armor units and tests comparing stable beach profiles with stable breakwater profiles developed by the action of an infinite number of waves.

The result of the combined research is the suggestion of a profile which includes two impermeable sheets or membranes each serving its particular purpose of increasing the stability of the rubble mound. Units should be placed with the longest side perpendicular to the slope which should be S-shaped with the slope in the area of wave breaking.

It was convenient to publish the paper in two parts, each dealing with separate problems. Figures and tables are numbered in consecutive order. Each part has its own list of reference literature and list of notations used. The discussion and conclusion in Part II refer to the results of both parts. The research is being continued with emphasis on the resonance phenomenon between downrush period and wave period which appears to be critical for structural stability.

## REVIEW OF FORCES ON AN ARMOR UNIT PLACED IN A RUBBLE STRUCTURE

A unit placed in a breakwater in contact with other units is subjected to forces by breaking waves, wave uprush and downrush. During the action the structure is, to a certain extent, filled with water which exerts hydrostatic pressures on the armor unit. Understandably, it is very difficult to analyse such a problem in all three dimensions. When wave action is assumed to be perpendicular to the face of the structure, the hydrodynamic forces are mainly two-dimensional, but forces on the units are still three-dimensional. To facilitate the analyses all forces introductorily are at first considered being two-dimensional. This simplifying assumption may cause some errors but will hardly affect the appraisal of the relative importance of the forces involved.

The literature includes a great number of papers on the stability of rubble structures built of armor units whether natural rock or concrete units. Several design formulas exist (10, 11) but relatively little has been done to explain the reasons for failures. Efforts have rather been put in to defining "design waves" (e.g. 2) with reference to wave height only - not to periods. An exemption is a recent publication from CERC (6) which includes period. While the overall stability of rubble structures has been studied extensively with regular as well as irregular waves (e.g. 5, 8, 9) little has been done to study detailed structure hydrodynamics.

One of the most detailed analyses of forces acting on a rubble structure was undertaken by Sigurdsson (20). To simplify the problem Sigurdsson considered balls of equal geometry, but he only measured total forces perpendicular and parallel to the slope. No attempt was made to analyse forces in relation to the stability of the structure as a whole and no recording of the time relation between external and internal waterlevels were made thus enabling an analysis

of the corresponding forces and the importance of porosity.

Table 1 is a review of acting forces. Some of these forces are destructive only, others are stabilizing and some may be either one - depending upon their direction at any particular moment.

TABLE 1 FORCES ACTING ON ARMOR UNITS OF  
DIAMETER, D, AND DENSITY,  $\rho_s$

FORCE	IDENTIFICATION CODE
Gravity	$G = \rho_s g \frac{\pi D^3}{6}$
Buoyancy in liquid of density, $\rho_w$	$B = \rho_w g \frac{\pi D^3}{6}$
Breaker, Uprush and Downrush Forces:	
Parallel or normal Forces	
Pressure Forces on Object (u = velocity of water)	$F_p = \rho_w \frac{\pi D^3}{6} \frac{du}{dt}$
Pressure Forces by "added mass" ( $C_m$ = added mass coefficient)	$F_I = C_m \rho_w \frac{\pi D^3}{6} \frac{du}{dt}$
Forces by shear (drag) ( $C_D$ = drag coefficient)	$F_D = C_D \rho_w \frac{\pi D^2}{8} u^2$
Lift Forces on Object	$F_L = C_L \rho_w \frac{\pi D^2}{8} u^2$

#### DETAILED DISCUSSION OF REASONS FOR FAILURE

Factors influencing stability include:

- (a) uprush and downrush velocities and the corresponding forces
- (b) the permeability of armor, sublayer and core
- (c) the friction between armor units and between and sublayer

This includes placement of units.

These forces may be studied by observing the location and pattern of failure.

Location of failure - Model tests (5, 12, 20) demonstrated that failures at idealized sphere mounds occur at or below the lowest level of wave retreat due to high normal forces. In the case of quarystone rubble mound with pell-mell placement, conditions are quite different. Fig. 1 shows the damage distribution curves based on extensive test series (14). Damage started and was most pronounced just below the S.W.L. where maximum downrush velocities occur.

Pattern of failure - Comprehensive investigations (14) verified that the fluctuating pressure due to up- and downrush caused slumping of the armor layer below the S.W.L., resulting in closely packed armor units. At and above the S.W.L. armor units become less compact. Some units in this area may become entirely dislodged from the face of the structure (Fig. 2a) and roll down the slope (Fig. 2b).

#### UPRUSH AND DOWNRUSH

Various authors have discussed uprush and downrush, some of these discussions are theoretical and others are based on experimental results. The classic papers by Miche (17, 18) refer only to regular waves, as does that of LeMéhauté et al (15). Recent investigations by Battjes (1) present results on wave uprush with irregular waves. Laboratory experiments, with and without wind waves, offer a great number of results which are not always applicable to prototype structures.

Theories (3) have also been attempted on downrush based on semi-theoretical flow conditions considering downrush under similar basic hydraulic laws on friction as stream flow. The approach to be discussed does not involve any other basic hydrodynamic law than the equation of continuity.

Fig. 3 shows up- and downrush profiles recorded on film at various time increments. The average velocity at the S.W.L., parallel to the slope ( $v_p$ ) and the velocity of the water surface perpendicular to the slope at the S.W.L. ( $v_n$ ) was

computed (4). During downrush the slope of the water table increases ( $\beta$  decreases) until the water surface due to friction and outflow from the breakwater body is parallel to the rubble mound slope (curves 4 and 5 in Fig. 3). The boundary conditions shown in Fig. 4a are chosen for calculation of velocities at the S.W.L. The average velocity in the cross-section A-B in 4a may then be expressed as:

$$V_p = \frac{\partial r}{\partial t} + \frac{r^2}{y_0 + r \tan \beta} \cdot \frac{1}{2 \cos^2 \beta} \cdot \frac{\partial \beta}{\partial t} = V_p(r) + V_p(\beta) \quad (1)$$

where  $V_p(r)$  and  $V_p(\beta)$  are the velocities due to changes in  $r$  and  $\beta$  respectively (see Fig. 4a).

The velocity of the water surface perpendicular to the slope may, according to (4), be written as:

$$V_n = r \cdot \frac{\partial \beta}{\partial t} \quad (\text{Fig. 4a}) \quad (2)$$

where the  $\beta$ -distribution curve and its assumed extension is indicated in Fig. 5.  $d\beta/dt$  approaches zero as  $\beta$  approaches zero leading to the following boundary limits:

$$\lim_{\substack{\beta \rightarrow 0 \\ \partial \beta / \partial t \rightarrow 0}} |V_p| = \frac{\partial r}{\partial t} \quad (3)$$

approaching a slope parallel flow (Fig. 4b) which neither becomes zero nor infinite. Curves for  $y_0 = 0.5$  and 2 cm are stipulated in Fig. 6.

Evaluation of flow conditions and forces based on laboratory experiments - To obtain a better understanding of "rubble structure hydraulics", experiments were carried out on a mound composed of spheres. Some of these tests (Fig. 7) by which forces on a sphere were measured are described in (22). It was noted that for uprush the total slope parallel force  $F_p = F_D(\text{drag}) + F_I(\text{inertia})$  maximized shortly after the spheres submerged, while  $V_p$  and the corresponding acceleration



maximized a little later (see  $F_p$  and  $F_I$  for test series 1 in Fig. 8). During downrush  $F_p$  maximized as the balls emerged. At that time downward maximum velocities occur while deceleration of the flow is still low. This, however, is only true for locations above the "incipient breaker-backwash zone" or for zone 1 in Fig. 9. Farther down,  $F_p$  increases due to the rotating velocity vectors at the toe of the incoming wave. One may therefore divide the exposed rubble slope into two main zones (Fig. 9). In zone 1, velocity and acceleration are mainly parallel to the slope. In zone 2, the velocity field changes suddenly and the quasi-hydrostatic pressure in the structure develops rapidly when the downrush plunges into the following wave. This causes a strong flow component perpendicular to the slope, resulting in considerable acceleration forces, particularly when resonance between the uprush/downrush period and the wave period occurs. During recent tests (12) two pressure gauges were installed at either side of a sphere located just below the S.W.L., Fig. 10. The results of these tests as shown in Fig. 11, demonstrate the connection between the quasi hydrostatic pressure  $P_0(A)/\gamma$  = the rise of the water above the S.W.L. at A and the total pressure measured (curves 1 and 3 in Fig. 11). It therefore indicates the nature of the acting forces. In addition, the pressure distribution between gauges A and B (curves 1 and 2) is given in Fig. 12. The quasi hydrostatic pressure curve (3' in Fig. 11) was calculated as  $P_{st}/\gamma = P_3/\gamma \cdot \cos(\alpha/\beta)$  where  $\alpha$  is the breaker-water slope,  $\beta$  = the angle between the slope and the water surface and  $P_3 = \gamma h + P_0(A)$  is the elevation of the water surface above gauge A. From Fig. 11 it is apparent that the dynamic pressure at A,  $(P_1 - P_{st})$ , during the first phase of the uprush, is minor (non-breaking waves). The  $\beta$ -distribution, however, is only known during downrush (Figs. 5 and 6). During uprush, as well as during the first phase of downrush, the calculated piezometer pressure becomes slightly higher than the pressure measured at gauge A (see the first record in Fig. 11), indicating that point A lies close to or

even below the separation zone (Fig. 13). This pressure difference, caused by suction, is probably of minor importance. It disappears before exposure of the sphere. The pressure differences between points B and A (defined as positive outward from the slope) is given by the pressure difference between curves 2 and 1 (Fig. 12). As mentioned above, the dynamic pressure during uprush seems to be minor only. It therefore is reasonable to conclude that the rather small inward directed pressure difference ( $\Delta p_1 \div \Delta p_2$ ), occurring in less than 0.1 sec (Fig. 12), is a result of delay in the built up of hydrostatic pressure at point B in the mound. Later during the uprush, and until the arrival of the next wave, considerable outward pressure differences occur during approximately 1.3 sec, maximizing during the exposure. To understand this better let us look at the situation occurring 1.4 sec from the start of recording (point C in Fig. 12). The measured pressure difference was then  $(\Delta p_2 \div \Delta p_1) / \gamma = 2.5$  cm. The hydrostatic pressure difference between gauges 1 and 2 due to the sloping water table (Fig. 13) may be calculated as  $\Delta h = D \sin(\alpha \div \beta) = 2.8$  cm which is even higher than the pressure measured. This indicated that the outward directed pressure difference during the downrush generally is related to the sloping water table and to a less extent to the fact that point A on the sphere is located close to the separation zone (Fig. 14). In the case of an even placed cover layer the uplift from the downrush must therefore be related to the hydrostatic pressure difference due to the sloping water surface.

In discussing the flow conditions on a rubble mound slope it is proper to first define various flow conditions:

- a) Outflow (curve 2 in Fig. 3) starts in the lower-most part of the structure slope during the latter stages of uprush due to build up of quasi hydrostatic pressure resulting from the sloping water surface.
- b) Backflow is outflow + drain water from the structure which flows down the exposed armor slope.

- c) Inflow into the structure takes place during uprush and is maximized below or close to the crest of the advancing wave or uprush.

The oscillating flow on a slope exposed to nonbreaking waves may be described as follows:

Phase 1 At the lowest level of wave retreat the backflow either plunges into the advancing wave or it penetrates deep downslope before uprush by the next wave starts. In either case, a complex flow situation occurs, as described below. Forces directed outward from the slope dominate.

Phase 2 Higher upslope, the uprushing wave meets the outflow from the structure that still submerges the armor units.

Phase 3 Still higher upslope, impact forces occur when the uprush strikes an exposed block (this may occur between curves 8 and 9 in Fig. 3b).

During phases 2 and 3 inflow takes place and uplift, drag and inertia forces are induced. Uprush gradually thins out and the flow into the structure is gradually limited to the upper part of the uprush while further downslope outflow starts, due to the sloping water surface as described above. This is mainly noted for higher void ratios of the core material.

Phase 4 Downrush starts followed by backwash. The elements in the slope are then subjected to uplift, drag and buoyancy-forces. Parallel forces dominate. Fig. 15 shows the flow conditions late in the downrush phase. Wave profile characteristics and extreme force situations are shown in Fig. 16. Combining this figure with Tables 2 and 3 gives the respective forces for various locations of a sphere on the slope.

TABLE 2 POINTS OF FORCE RECORDS (FIG. 16)

	Condition Number (See Fig. 16)						
	1	2	3	4	5	6	7
Z/D	0.71	0.71	1.38	2.12	2.13	2.84	4.27
H/D	2.60	2.37	2.42	3.22	2.65	2.36	1.84
T	1.72	1.72	1.69	1.71	1.69	1.75	1.69

TABLE 3 CHARACTER OF FLOW SITUATION (FIG. 16)

		Condition Number (See Fig. 16)						
		1	2	3	4	5	6	7
Uprush	F <sub>p</sub>	d	c,f	c	c	c	b	b,e
	F <sub>n</sub>	f	c,f	c,f	c,f	f	f	f
Downrush	F <sub>p</sub>	a,g	a,g	a	a	a	a	e
	F <sub>n</sub>	a,g	a,g	a	a	a	a	a

Table 3 also compares flow conditions for different locations on the breakwater slope for the seven tests indicated in Fig. 16.

- a: Outflow
- b: Incipient breaker preceded by backflow
- c: Incipient breaker preceded by outflow
- d: Impact
- e: Backflow
- f: Inflow
- g: Change in buoyancy

The zero level for forces corresponds to a situation with only hydrostatic forces acting upon the sphere (no wave action). This, in turn, means that for a sphere located below the S.W.L. the values for  $F_p$  and  $F_n$  are negative when the unit becomes exposed, while in case of a unit located above the S.W.L. positive values for  $F_p$  and  $F_n$

occur when the unit is submerged. The phase angles  $0^\circ$  to  $360^\circ$  correlate the force records with the passing of the wave crest over the monitored sphere.

It should be noted that, in a highly permeable structure such as a rubble mound, an important part of the downrush takes place through the pores in the armor and sublayer while outwash from the mound takes place simultaneously - making it very difficult to distinguish between downrush and outflow. However, one may obtain a good understanding of the flow conditions by examining the configuration of the water wedge as it develops and compare this with the force pattern diagrams in Fig. 16. Inflow starts and is maximized as units are submerged at which time  $F_p$  is almost zero ( $t_p = 0^\circ$ , tests 2-6, Fig. 16) while  $F_n$  first is definitely negative. Shortly after, it is minimized and does not become zero until approximately  $0.23T$  sec later ( $t = t_p + 0.23T$ ). This is to be expected and is in agreement with the above mentioned tests (12) because it takes time to fill the pores of the structure. The timing of the force distribution in Fig. 16, however, is somewhat impractical as the time of the occurrence of the maximum water pressure varies along the slope making comparisons along the slope complicated. One may divide the water surface in two zones, D'-E and E-F' respectively (Fig. 3b). Below point E the water surface reaches its maximum elevation at time  $t_p = (8)$ , corresponding to curve 8, while maximum elevation first occurs sometime later above E (e.g.  $|t_p = (8)| - |t_p = (9)|$  corresponding to curve 9). This means that outflow for elevations below the S.W.L. already starts during the latest phase of uprush while inflow is maximized farther up - causing a circulating in- and outflow as indicated in Fig. 17. Future timing of forces during tests should probably be more practical.

The dislodging forces, whether inertia or drag and lift forces, should be minimum. Maximum inertia forces parallel to the slope occur in the upper part of the slope where velocities are small and drag forces consequently small too.

Another area where high slope-parallel inertia forces may occur is where the breaking wave hits the slope. Here velocities and accelerations are pointed somewhat downwards towards the slope. Drag and lift forces are maximum where velocities are maximum which as it may be seen from Fig. 6 is not necessarily the lowest point of downrush - but may be at a point further upslope. They are highly dependent upon the geometrical shape of the unit. On the basis of analyses on coefficients of inertia and drag (7, 13) it may be concluded that - disregarding the influence of permeability - a streamlined shape of the exposed side of an armor unit increases stability, regardless of the fact that average downrush velocities (and accelerations) may increase slightly. This may also be caused by the fact that streamlined geometry causes relatively less turbulence and turbulence increases all forces. With respect to forces by flow perpendicular to the slope, velocities are generally small, which decreases the importance of geometrical shape.

#### THE IMPORTANCE OF POROSITY (PERMEABILITY)

Another important factor in the stability of a rubble structure is the porosity of the armor, underlayers, core and filter material. This is a determining factor in the intensity of out- and inflow, as well as for the elevation of the water surface within the breakwater core - later referred to as the GW-level. For very fine core material the water surface within the structure is located almost at the elevation of maximum uprush, while for very coarse material the water surface oscillates with and tends to follow the up- and downrush.

To examine the nature of the outflow more closely a flow net was sketched (Fig. 18) for a wave condition just prior to breaking, assuming quasi stationary conditions for a fraction of a second. A model (Fig. 19) may provide the detailed information needed to determine the distribution of flow gradients for calculations of pressure and velocity

fields. The flow net reveals that the outflow is concentrated at the lowest level of wave retreat causing strong normal forces. In the cover and sublayer maximum outflow velocities follow the wave action rather closely, maximizing  $F_n$  just before the wave trough passes ( $F_{n_1}$  in Fig. 15 and Fig. 16 - tests 5 and 6). Further upslope, when armor units are partly exposed during the backrush,  $F_n$  is maximized just as the top of the armor unit is exposed ( $F_{n_2}$  in Figs. 15 and 16 - tests 1 and 2). Simultaneously  $F_n$  is maximized while  $F_p$  minimizes. Drainwater from the structure flows around the units in a thin high-velocity sheet. This situation occurs when the wave has retreated to below the top of the unit ( $F_{p_1}$  in Figs. 15 and 16 - tests 1 and 2). In both cases outflow velocities are essentially normal to the structure slope. The effect of the outflow on  $F_p$  is only felt to a depth slightly below the lowest level of wave retreat. Further down-slope,  $F_p$  is minimized due to the backflow ( $F_{p_3}$  in Figs. 15 and 16 - test 7), while  $F_n$  is maximized. This combination of forces may cause units to be removed from their position in the slope.

If the incipient breaking is preceeded by outflow,  $F_p$  is directed upslope, which is a less dangerous situation for steep structure slopes. The situation is the opposite if the incipient breaker is preceeded by backflow. A better understanding of the flow conditions may be gained by reviewing the velocity field within a breaking wave (Figs. 20a and 20b). While high forward velocities dominate in the crest, velocities are opposite in the lower part of the wave. The rapid change in direction of velocities in the toe (lower part) of the wave, causes high acceleration fields. The condition is similar when a wave breaks on a sloping structure where downrush and outward velocities in the toe combine as indicated in Fig. 21. When downrush velocities join upward velocities in the back part of the toe, the combined velocity vectors rotate causing high accelerations. This ultimately results in a broad sustained maximum of  $F_p$ , reaching a peak value as the

velocity vectors are directed almost normal to the breakwater slope. At the same time  $F_n$  is maximized. This situation may be expressed as follows:

$$F_n(\max) = f(V_n^2, \dot{V}_n, B, i, P_{gr}) \quad (4)$$

$$F_p(\max) = f_2(V_p^2, \dot{V}_p, B) \quad (5)$$

where  $V_n$  is the velocity perpendicular to the slope intensified by outflow from the core (Fig. 21),  $B$  is the buoyancy force,  $i$  is the flow gradient and  $P_{gr}$  is the grain pressure in the core just below the filter layer.  $\dot{V}_p$  may be expressed  $\dot{V}_p = \dot{r}\dot{\phi} + r\ddot{\phi}$  where  $r$  is the radius of curvature of a fluid particle and  $\phi$  is the angle between the  $r$ -line to the water particle and the breakwater slope as indicated in Fig. 21, (one dot indicates the first, two dots the second derivative).

Fig. 22 (ref. 20) shows typical force diagrams for the condition when the incipient breaker is preceded by backflow. The similarity to those in Fig. 16 - tests 6 and 7 - may be noted although outflow is less pronounced. Furthermore it is interesting to note that the increase in  $F_n$  due to intensified outflow from the interior fill or core (Fig. 22 a) - although still relatively low - results in a more sustained peak.

When the incipient breaker is preceded by outflow an important part of the backwash takes place through the armor and its sublayer. When the breaking wave meets this flow a similar change in the parallel velocity field occurs as in the case of an incipient breaker preceded by backflow. Velocity and acceleration fields are essentially normal to the slope maximizing  $F_n$ . This situation occurs as the armor unit is submerged just before the front of the breaker passes.

Maximum inflow takes place under or close to the crest.

This minimizes  $F_n$ . In the case of outflow  $F_n$  is maximized before  $F_p$  reaches its maximum value. In the case of incipient breaker preceded by backflow,  $F_n$  and  $F_p$  are maximized at the same time. Generally,  $F_n$  is maximized by incipient breaker preceded by outflow or by a change in the buoyancy force and reaches a peak at or below the lowest level of wave retreat.



Impact forces may occur when the breaker front strikes an exposed unit just before the unit is submerged (Fig. 21, zone C) causing an instantaneous rise in  $F_p$  which may move the ball.

Below the incipient breaker zone outflow from the structure becomes the primary effect for the normal forces. The open core section intensifies outflow and changes the shape of the force distribution curves primarily by affecting  $F_n$  above and below the peak value. The width of the peaks, which in the case of an "open core" occurs farther downslope, increases with increasing wave length. In the case of a flatter slope uprush and downrush are both less. For detailed information the reader is referred to reference 20 where results, however, suffer from the fact that time history of forces and water surface movement are not measured continuously and simultaneously. The conclusion which may be drawn from the above mentioned results is that the highest  $F_n$  occurs close to the lowest level of wave retreat simultaneously as  $F_p$  is maximized. This is in agreement with observations in a number of hydraulic model tests with spheres composing the cover layer.

As the influence of outflow on the stability is still uncertain, an attempt was made to clarify the relative magnitude of the internal forces by laboratory experiments (16). A rubble mound structure was built. As cover layer, spheres weighing 48 grams and granite stones weighing 140 grams were used respectively. The filter consisted of granite pebble (5 grams) while core material consisted of 4.7 - 9.4 mm marble chips. The structure slope was 1 in 1.5. Between the armor and the sublayer various membranes were placed extending down to different elevations. Three different membranes were used, perforated steel, impermeable steel plate and impermeable plastic sheet. The results of these tests are shown in Fig. 23 and are described in detail below.

In the first place it is noted that there was a very abrupt drop in height of waves causing failure when the plastic

sheet was extended down to a certain depth below S.W.L. For all alternatives tested, failure occurred at maximum downrush.

(1) Permeable steel plate between armor and sublayer.

As the permeability of the plate matched the permeability of the core material, it could be expected that this would not influence the inflow - outflow situation. The hydrostatic pressures from the inside would therefore remain the same. The spheres, however, have a more even base to rest on. As shown in the Table included in Fig. 23, failure under these conditions (Fig. 23,a) occurred for wave height of 7.5 cm.

(2) Impermeable rigid steel plate. As the plate reached above the level of maximum uprush, the out- and inflow was limited to zone  $l_b$  in Fig. 23,b. The water level in the structure stayed just above the S.W.L. instead of at elevation approximately  $R_u/2$  (Fig. 18) above the S.W.L. as for fully permeable tests conditions. If the internal forces are of some significance, the stability could be expected as was the case to decrease when the steel plate is gradually moved downslope and the outflow becomes more concentrated. The stability did minimize when the steel plate reached a position just below maximum downrush (Fig. 23,b2). The outflow was highly concentrated at the same time and place as the external forces were maximized. This resulted in a 10% reduction of wave height causing failure. As the steel plate was extended further down the slope, the stability increased again since the plate entirely prevented outflow (Fig. 23,b3).

(3) In the case of an impermeable flexible plastic sheet, the same trend as above was noted and the plastic sheet did not influence the stability conditions noticeably until it reached down below a certain elevation. At this point the wave height causing failure suddenly decreased approximately 50% (see Table in Fig. 23).

To explain this, consider a dam with a thin asphalt or ice cover (Fig. 23,d). A certain drop in water level would induce

a build up of hydrostatic pressure from the inside. In this particular case, concrete balls of 48 grams placed on a 1:1.5 slope exert normal stabilizing pressure of  $4.03 \text{ g/cm}^2$ . Thus theoretical failure should occur if the outside water level dropped 4 cm or more, as would be the case during downrush.

Comparing this to the tests with plastic sheets, failure did occur for a wave height of 4 cm as the plastic sheet reached down to 10 cm below the S.W.L. The lowest level of wave retreat was 2.7 cm. As the water level in the structure was approximately 0.7 cm above the S.W.L., this resulted in maximum hydrostatic pressure of  $3.4 \text{ g/cm}^2$  if fully mobilized - which is more than 85% of the pressure needed to displace the balls (Fig. 23,c).

Fig. 24 shows the condition at maximum downrush with the same ratio between maximum downrush and the elevation of the GW-level as in Fig. 23,c. Point A is the point where theoretically outflow turns into inflow. In this case it is located 7.8 cm below the lowest level of wave retreat. Using the wave profile shown by dotted lines, the equivalent point A1 could be located still farther down, or somewhere between elevation -7.5 cm and -10 cm, as also found in the tests. When the plastic sheet reached down to or below point A, the wave height causing failure was constant and very low, due to the build-up of quasi-hydrostatic pressure from the inside. The location of this out-inflow points therefore depends upon the elevation of water table in the core (that means the permeability of the core), wave steepness and wave height.

The sudden reduction in wave height causing failure deserves still more detailed explanation. As indicated, the wave height causing failure dropped from 8 cm to 4 cm when the plastic sheet reached down to approximately 8 cm below S.W.L. This means that point A for this particular wave condition ( $H=8 \text{ cm}$ ) was located at distance  $-H$  below S.W.L. First when the plastic sheet reached to this point, hydrostatic pressure built up high enough to cause failure. If a permeable steel

plate is placed between the armor and filter layer, the relationship between the normal forces causing failure and the wave height is likely to follow curve 1 in Fig. 25. Curve 2 applies when the plastic sheet extends below the point of outflow where  $L/H > L_A/H_A$  as defined in Fig. 25. It may be noted that  $L_A/H_A$  for the conditions tested was constant and approximately equal to one for the same steepness of the waves at breaking. For increasing steepness the point of outflow moves upslope (Fig. 24) for constant wave height at breaking. Assuming as an illustration that a plastic sheet extends down to -6 cm, starting with a low wave height and increasing it gradually the forces exerted upon the cover layer follow curve 2 until  $H \sim 6$  cm, then drops to curve 1 when point A comes below the plastic sheet. The opposite development takes place when  $H$  starts  $> 6$  cm and then decreases. Initially, the force follows curve 1 until  $H=6$  cm and then jumps up to curve 2.

This situation is of importance for coastal protection which includes impermeable mattresses of any kind as well as the case of impermeable ice sheets which may form on a rubble mound structure.

The influence of permeability - The influence of different permeability of the core material on the stability of a breakwater, seems rather uncertain. The forces from the core ( $F_{core}$ ) which influence stability, may be defined as:

$$F_{core} = F(v_c^2) + F(i_c) \quad \text{where } v_c^2 = p \cdot i_c \quad (6)$$

$p$  is the permeability of the core material,  $v_c$  is the velocity of the water outflow from the core and  $i_c$  is the pressure gradient. The problem is to determine the porosity that minimizes  $F_{core}$ .

To investigate the importance of permeability on stability, tests were run (21) using the same armor layer (6 cm granite rock) and the same filter layer (2-3 cm stone), but with three different sizes of core material and wooden slab as

the fourth alternative. The water elevation within the structure measured at the time of maximum wave run up is shown in Fig. 26. For very low permeabilities, the highest water elevation occurred after maximum uprush in the core just inside the sublayer and slightly below the position of maximum uprush. For low permeability, hydrostatic pressure builds up in the core during wave withdrawal:  $F(i_c)$  is high,  $F(v_c)$  low. The combined pressures maximized at maximum downrush where the external conditions, too, are most critical. For high permeability of the core, the situation reversed, because the water level in the structure followed the retreating wave more closely.

Hedar (10) and Hudson (11) found a considerable increase in stability for high permeability of the core material. Fig. 27 (14) shows the damage ratio plotted against the wave height for various core material. It demonstrated that damage was more pronounced and occurred earlier with finer core material than with a coarser core. This is particularly noticeable for higher damage ratios. Stability, within certain limits, therefore seems to increase with increasing permeability:  $F(i_c)$  reduces more than  $F(v_c)$  increases. A damage diagram mentioned in part II of this paper with reference to Fig. 41, substantiates this and indicates how stability decreases due to build-up of hydrostatic pressure if outflow is prevented. Test series I with a wood slab below the filter is supposed to simulate an impervious core (Fig. 28 a). As the wood slab eliminates all effects from the core,  $F_{core} = F(v_c^2) + F(i_c) = 0$ .  $F(i_c)$  maximizes when the void ratio becomes very low and stability decreases when permeability ( $p$ ) decreases (tests II, III, IV in Fig. 27). This means that  $F_{core}$  increases, resulting in a stability condition similar to alternative I for  $p=0$  (wood slab, Fig. 28 a).  $F_{core}$  therefore is not maximized, but zero's. The reduced stability experiment with a slab below the filter layer may, as discussed later, be related to a reduced angle of repose and a more intensified backwash in the zone between the wood slab and the filter layer.

Sigurdsson (20) measured the forces on spheres in a 1 in 1.5 slope armor layer for two test series with different core material. Sigurdsson's core material partly used an impervious wood slab (series B) and partly an open core (series A) and found that in the case of an open core the intensified outflow increased the value of the maximum normal forces above and below the peak of the distribution curves. The peaks of the force distribution curves were therefore much more abrupt (steep) for series B than for series A. This may be noted by looking at the general equation for the maximal normal force  $F_n$  per unit volume ( $\bar{V}$ ) given by Sigurdsson as:

$$F_n/\gamma_f \cdot \bar{V} = \cos\alpha + \lambda H/D \quad (7)$$

where  $\lambda$  is an experimentally determined coefficient which appears to increase somewhat with increasing steepness of the structure and with increasing permeability of the structure core (decreased stability).  $H$  is wave height and  $D$  = diameter of sphere. The slight increase in  $F_n$  in the case of the wood slab indicates that the increase in drag and inertia forces on the filter and armor units for the model tested (Fig. 28 b) is only small.  $F(i_c)$ , however, may be of significant magnitude as evidenced by test series II, III, IV (Fig. 27). The water level at maximum up- and downrush are indicated in Fig. 28 b. It is likely that such conditions will cause higher normal forces at a lower level of wave retreat than measured by Sigurdsson, whose results only provide a trend. Comparing Sigurdsson's results and the damage diagram in Fig. 27 (4, 14), a distribution curve for forces due to inside pressure in the core versus permeability was sketched in Fig. 29. Within certain limits of permeability of the core material compared to the permeability of armor and sublayer, the stability is almost unaffected by small changes in permeability.

## DISCUSSION AND CONCLUSION

### THE RESONANCE PHENOMENON

From the above mentioned analyses it is obvious that the destructive forces may develop maximum size at two different places on the rock slope. One is where downrush velocities are maximum and therefore cause maximum slope parallel as well as slope perpendicular forces. This is not when downrush is in its lowest position but before then. The other is when downrush velocities, even if they are lower than maximum velocities, join with suction (lift) forces occurring in the toe of a breaking wave causing what may be called a "resonance" maximizing hydrostatic pressure from the core structure at the same time. Such situation may occur if the uprush-downrush period or what may be termed the downrush period is equal to the wave period, assuming that downrush is at its lowest position at the toe of the breaking wave so that every downrush meets a breaking wave at the lowest position of the downrush. In an irregular sea this should be put in relation to the wave spectrum and its sequence of waves. The design of stable rubble mound structures may consider these two possibilities by providing a relatively gentle slope where downrush velocities are high or maximum causing high inertia, lift and drag forces. This area includes the area where hydrostatic forces may join the combined forces by downrush and toe suction resulting from resonance between uprush-downrush period (with downrush in its lowest position) and wave period. The practical design aspects of these problems are elaborated in the "Discussion and Summary" of Part II, which combines all results mentioned in Parts I and II.

## REFERENCES

1. Battjes, J.A., "Run-Up Distribution of Waves Breaking on Slopes", Journal of the Waterways, Harbors and Coastal Engineering Division, ASCE, Vol. 97, No. WW1, Proc. Paper 7923, Febr. 1971, pp. 91-114. See also Battjes' "Computation of Set-up, Longshore Currents, Run-up and Overtopping due to wind-generated Waves", Doctoral thesis at the Technical University at Delft, Holland, 1974.
2. Bretchnneider, C.L. and Reid, R.D., "Surface waves and offshore structures", Texas A. And M. Research Foundation Technical Report, October 1953.
3. Brandtzæg, A. and Tørum, A., "A simple mathematical model of wave motion on a rubble mound breakwater front", Proceedings, the Xth Conference on Coastal Engineering in Tokyo, Chapter 26, 1966.
4. Bruun, P.M., "Damage functions of rubble mound breakwaters". Discussion in Waterways and Harbors Division, ASCE, Vol. 96, No. WW2, Proc. Paper 6743, pp. 559-568, May 1970.
5. Carstens et al, "The Stability of Rubble Mound Breakwaters against Irregular Waves", the Xth Conference on Coastal Engineering, Tokyo, Chapter 55, 1966.
6. Coastal Engineering Research Center, U.S. Army Corps of Engineers, Washington, D.C., "Rip rap stability on earth embankments tested in large and small scale", Technical Memorandum No. 37, 1972.
7. Chepil, W.S., "The Use of Spheres to Measure Lift and Drag on Wind Eroded Soil Grains", Proceedings Soil Science Society of America. Vol. 25, No. 3, 1961.
8. Gaillard, D.D., "Wave Action in Relation to Engineering Structures", Fort Belvoir, 1904, 2 ed. 1935, Repr. 1945.
9. Galvin, C.J., "Breaker Travel and Choice of Design Wave Height", Journal of Waterways and Harbors Division, ASCE, Vol. 95, No. WW2, Proc. Paper 68, May 1969, pp. 175-200.
10. Hedar, P.A., "Stability of Rock-fill Breakwaters", Akademiförlaget-Gumperts, Gøteborg 1960.
11. Hudson, R.Y., "Laboratory Investigation of Rubble Mound Breakwaters", Transactions of the ASCE, 1961, Vol. 126, Part IV, pp. 492-541.



12. Johannesson, P. and Bruun, P.M., "Hydraulic Performance of Rubble Mound Breakwaters. Reasons for Failure", Proceedings, the First International Conference on Port and Ocean Engineering under Arctic Condition, Vol. 1, pp. 326-359, the Norwegian Institute of Technology, Trondheim, Norway 1971.
13. Kamphuis, J.W., "A Mathematical model to advance the understanding of the Factors involved in the Movement of Bottom Sediment by Wave Action". C.E. Research Report No. 53, March 1966. Civil Engineering Department, Queen's University at Kingston, Ontario.
14. Kydland, O., "Stabilitet av rausmoloer" - (Stability of rubble mound jetties). Thesis for the degree of Licentiatu Technicae, Main Library of the Norwegian Institute of Technology, Trondheim, Norway 1966. (Norwegian text).
15. LeMéhauté, B. et al, "A Synthesis on Wave Run-up", Journal of the Waterways and Harbors Division, ASCE, Vol. 94, No. WW1, Proc. Paper 5807, February 1968, pp. 77-92.
16. Loe, H., "The Influence of Impermeable Sheets Placed Below the Armour on the Stability of Rubble Mounds". The Norwegian Institute of Technology, Dept. of Port and Ocean Engineering, Trondheim, Norway. (Unpublished report, Norwegian text).
17. Miche, A., "Pouvoir Réfléchissant des Ouvrages Maritimes Exposés à l'Action de Houle", Annales des Ponts et Chaussées, Vol. 121, 1951.
18. Miche, M., "Mouvements Ondulatoires de la Mer en Profondeur Constante ou Décroissante", Annales des Ponts et Chaussées, Memoires et Documents 114e Anne, Paris 1944.
19. Miller, R.L. and Zeigler, J.M., "The Internal Velocity Field in Breaking Waves". Ninth Conference of Coastal Engineering, Lisbon, Portugal 1964, Chapter 7.
20. Sigurdsson, G., "Wave forces on breakwater capstones". Journal Waterways and Harbors Division, ASCE, Vol. 88, No. WW3, Proc. Paper 3218, August 1962, pp. 27-60.
21. Sodefjeld, A.T., "Innvirkning av dekkblokkenes spesifikke vekt på stabiliteten av rausmoloer med fronthelning 1:1.5". (The influence on stability of the specific gravity of armor blocks). Unpublished report in Norwegian by the River and Harbor Laboratory, the Norwegian Institute of Technology, 1965.

22. Trøttestad, A., "Model Experiments to determine drag and mass coefficients for blocks on a breakwater slope", Unpublished report in Norwegian. The Norwegian Institute of Technology, 1966.

# A CRITICAL REVIEW OF THE HYDRAULICS OF RUBBLE MOUND STRUCTURES

## PART II

### FRICTION BETWEEN ARMOR BLOCKS AND BETWEEN ARMOR AND SUBLAYER SLOPE GEOMETRY

#### INTRODUCTION

Part II deals with the importance of friction in rubble mounds and with slope geometry. In order to analyse the problem of friction rationally it was necessary to idealize block geometry by considering spheres. The results therefore provide rather a "trend of development" but no other approach is possible as one otherwise would wind up with "hundreds of matrixes" and "thousands of combinations" which were hardly applicable in practical technology.

The results of the research is discussed and line of action on further research explained in addition to practical application of design principles discussed with contractors.

#### FRICTION FORCES

Although a theoretical approach to friction problems involves considerable difficulties, it was attempted to make some calculations for dry conditions assuming in the first place that only internal stabilizing forces are involved.

Consider an idealized rubble mound consisting of spheres of weight  $G$  placed on a base, with the same roughness as the spheres and with friction coefficient  $\mu$ . Assume further that just one horizontal row (No. 1 in Fig. 30) is affected by external force ( $F$ ) and by a moment ( $M$ ). The corresponding stabilizing forces are shown in Fig. 31. As the unknown forces total 6 and the equations of equilibrium only 4, one still needs 2 more equations. In addition it is assumed that one of the

three frictional forces are fully mobilized at the moment of failure. Viewing the model closely, it is apparent, however, that the contact pressure ( $T_2$ ) and the corresponding frictional force ( $F_1$ ) vanish at the moment of failure, leaving the system fully described by 4 equations only.

Consider first that the external force  $F$  acts perpendicular to the slope with angle  $\alpha$  with the horizontal making the following equilibrium equation for sphere No. 1 weight  $G$  (Fig. 32 a).

$$F_y(1) \leq G \cos\alpha + S_1 + S_2 \quad (8)$$

Equilibrium moment at points  $A_3$  and  $A_0$  on spheres No. 2 and 0 respectively (Fig. 32 a) gives:  $S_2(\max) = S_1(\max) = \frac{1}{2} G \cos\alpha$  (Fig. 32 a) or substituted into Eq. 8:

$$\underline{F_y(\max) = 2 G \cos\alpha} \quad (9)$$

$F_y$  may be explained as the maximal stabilizing force perpendicular to the slope acting through the center of the sphere. This may generally be expressed as  $F(\max) = 2 G \cos\alpha / \cos\beta$  (Fig. 32 b). The maximum moment  $M(\max)$  is determined similarly by equilibrium at point  $A_3$  and  $A_1$  (Fig. 32 c) or

$$\underline{M(\max) = G \cos\alpha \cdot D} \quad (10)$$

where  $D$  is the diameter of the sphere. Any arbitrary force causing failure, acting on the horizontal row of spheres, may therefore be written as  $F(\max) = G \cos\alpha \cdot D/\Delta$ . See Fig. 32 d where  $\Delta$  is defined. It remains to determine the number of spheres (rows) above the affected sphere which are necessary to prevent sliding between the balls and between the balls and the base.

As seen from Figs. 31 and 32,  $S_1 = S_2 = S_3 = 0.5 G \cos \alpha$  while  $F_1 = F_2 = 0$ . First one assumes that ball No. 3 ( $K=3$ ) is the uppermost ball (Fig. 33). Thus the following condition is required for equilibrium;  $\sum K_y(3) = 0$ ;  $T_3 = G \cos \alpha + S_3$ ,  $\sum M_C(3) = 0$ ;  $F_3 = S_3$ . No sliding at  $B_3$  requires that  $T_3 \cdot \mu \geq F_3$  while no sliding at A requires that  $(G \sin \alpha + F_3) \mu \geq S_3$  or combined:

$$F_3 = S_3 \leq G f(\alpha) \frac{\mu}{1-\mu} \quad (11)$$

where  $f(\alpha) = \min|\sin \alpha|$  and  $S_3 = \frac{1}{2} G \cos \alpha$ . This gives the following limits for roughness ( $\mu$ ) resulting in stable conditions with three balls only above the affected ball.

$$\mu \geq \frac{1}{1+2\operatorname{tg} \alpha} = \mu(\alpha) \quad \text{for } 0 < \operatorname{tg} \alpha \leq 1 \quad (12)$$

$$\mu > 1/3 \quad \text{for } \operatorname{tg} \alpha \geq 1 \quad (13)$$

The stability conditions are sketched schematically in Fig. 34 (line  $a_3 b_3 c_3$ ). In the case of less roughness of a certain mound slope, more spheres are necessary to obtain stability. The calculations below are based on similar boundary conditions. Due to lack of space only final expressions are given. The general requirements for stability are as follows:

$$F_{3+N} = S_{3+N} = \frac{1}{2} G \cos \alpha \frac{1-(2N+1)\mu}{1-\mu(-1)^N} \quad (14)$$

where

$$\mu = \frac{1}{(2N-1)+2\operatorname{tg} \alpha} = \mu(\alpha) \quad \text{for } 0 < \operatorname{tg} \alpha \leq 1 \quad (15)$$

$$\mu = \frac{1}{2N+1} \quad \text{for } \operatorname{tg} \alpha \geq 1 \quad (16)$$

These equations determine the number of balls (rows) necessary to prevent sliding. Failure will occur by the rolling of the 3 spheres (0, 1 and 2) out of their bed, where ball 1 (Fig. 31) is affected by external forces.

Consider as an example a 1 in 2 slope with concrete balls as cover layer placed on a concrete plate with the same roughness as the balls,  $\mu = 0.1$  (Fig. 35).

Eq. (15) gives the number of spheres above the exposed sphere (No. 1) necessary to resist the maximum external force ( $F_y = 2 G \cos \alpha$ ) by friction of the base. One has:  $2N - 1 + 2 \cdot 0.5 \geq 1/0.1$ ,  $N \geq 5$ . This reveals that maximum stability is obtained for ball No. 8 from the top. The maximum external forces causing failure will theoretically be constant for balls further down.

To clarify the importance of friction between cover and sublayer on the cover-layer's angle of repose (later referred to as  $\phi$ ) some dry tests were run. Filter blocks were glued to the wood slab (Fig. 36). The friction between cover and sublayer was changed by placing linen or plastic sheets as intermediate layers. The results are given in Table 4, where the average angle of repose,  $\phi$ , is a function of the contact friction (later referred to as  $\tau = \mu \sigma_N$ ) and the friction due to unevenness of the contact zone (column e in Table 4, later referred to as  $\sigma_p$ ,  $p$  = parallel to slope) or  $\phi = \phi(\tau) + \phi(\sigma_p)$ .

TABLE 4		Angle of repose $\phi$	Contact zone	$\phi(\tau)$	$\phi=\phi(\sigma_p)$
INTERMEDIATE LAYER					
	(a)	(b)	(c)	(d)	(e)
1	Linen sheet	59.5°	Stone/Linen	+	little more even (-)
2	Uneven surface	Directly on filter	52.7°	Stone/Stone	0
3	Plastic sheet	43.6°	Stone/Plastic		more even
4	Smooth surface	Wodden plate	37.6°	Stone/Wood	(+)
5	Perf. metal plate	35.2°	Stone/Metal	0	

These tests, however, did not record the friction ( $\tau = \mu \cdot \sigma_N$ ) between the armor stones and the intermediate layers. This would have required that the tests were divided in two series, one with an even stone plate below the intermediate layers and the other as described above. The first test series would then give  $\phi = \phi(\tau)$  and the second, which corresponds to the tests actually run and mentioned above, would give the increase of the angle of repose due to the unevenness in the contact zone  $\Delta\phi = \phi(\sigma_p)$ . Column d

of Table 4 gives an assumed trend of the  $\tau$ -distribution with the stone against stone surfaces as the reference level for friction.  $\tau$  is maximized in the case of the wet linen cloth probably because of adhesive forces. It is also possible that sharp edges on the cover stones may stick to the soft linen cloth.

The conclusion which may be drawn from these tests, is that the angle of repose increases with increasing friction ( $\mu$ ) as well as with increasing unevenness of the sublayer  $\phi(\sigma_p)$ . This might also apply to some extent in the case of wave action. This is in accordance with experiments run by Miller and Byrne (28). They found the following expression for the average angle of repose of a single particle on a rough bed:

$$\phi = f(\alpha, D/\bar{K}, \beta) \quad (17)$$

where  $\phi$  is the average angle of repose,  $\alpha$  is a parameter which incorporated the effect of shape and roundness in particle as well as bed,  $D/\bar{K}$  is the ratio of the diameter of a single grain to the average diameter of the bed grains and  $\beta$  is a parameter incorporating the effect of the sorting of the bed grains.

Miller and Byrne carried out their experiments using uniformly sized spheres of diameter  $D = 0.25$  mm. The results are indicated in Table 5 and in Fig. 37, which is a diagram showing  $\phi$  as a function of  $D/\bar{K}$  for various kinds of sand incl. spheres.

TABLE 5 ANGLE OF REPOSE OF INDIVIDUAL SPHERES ON FIXED BED OF UNIFORMLY SIZED SPHERES OF DIAMETER,  $K = .250$  mm

Particle Size D	.088 mm	.125	.175	.250	.350	.500	.710 mm
$\bar{\phi}$	72.4°	61.1°	52.5°	48.6°	38.5°	35.7°	29.0°
$\sigma_{\phi}$	16.9°	5.2°	14.0°	18.5°	19.0°	15.8°	9.7°
Tan $\bar{\phi}$	3.152	1.804	1.303	1.134	0.795	.719	0.554
$D/\bar{K}$	0.352	0.500	0.700	1.000	1.400	2.000	3.000

In all cases a relation

$$\phi = a (D/K)^{-0.3} \quad (18)$$

was found. The figure "a" varies and increases from 50 for

spheres to 70 for crushed quartzite. In Fig. 37 the popular ratios used for subsequent layers in rubble mound by U.S. Army Corps of Engineers standards have been added (ref. 25). They refer to weights which in Table 6 were converted to grain diameter ratios. The  $\phi$ 's corresponding to crushed quartzite (rubble mound block) are also listed in Table 6.

TABLE 6 POPULAR WEIGHT RATIOS IN RUBBLE MOUNDS AND THE CORRESPONDING RATIOS BETWEEN DIAMETERS IN ARMOR AND SUBLAYERS'  $\phi$ 'S AND  $\text{tg } \phi$  (APPROXIMATELY) FOR CRUSHED QUARTZITE

Weight ratios	Diameter ratios	$\phi$	$\text{tg } \phi$
W to W	1	$70^\circ$	2.75
W to W/2	1.25	$65^\circ$	2.1
W to W/10	2.15	$55^\circ$	1.4
W to W/20	2.7	$50^\circ$	1.2
W/2 to W/10	1.7	$60^\circ$	1.75
W/2 to W/20	2.15	$55^\circ$	1.4

It may be noted that the improvement of slope stability against sliding by the use of W/10 instead of W/20 as sublayer is  $1.4/1.2 = 1.15$ . The improvement of the stability by the use of a W/2 layer between the W and the W/10 layer is  $1.75/1.4 = 1.25$ . With respect to spheres, a peculiar situation seems to exist. Fig. 38 shows the relation between  $\text{tg } \phi$  as found by Miller and Byrne (28) and the number of contact points between the top spheres (armor blocks) and the sublayer spheres. Fully symmetrical and similar conditions with respect to placement of the spheres in two directions perpendicular to each other are assumed. The diameter of top armor spheres varies from 0.88 mm to 7.1 mm, the diameter of bottom (sublayer) spheres was 0.25 mm. It may be noted from Fig. 38 that there is an almost linear relationship between  $\text{tg } \phi$  and the number of contact points.

In Fig. 39 the number of contact points (A) is given as a function of grain diameters putting  $A = K/2.56$ . The following two relations were then found:



$$\operatorname{tg} \phi = \frac{K}{2.61} \quad \text{for } D/K < 1 \quad (19)$$

$$\operatorname{tg} \phi = \frac{1}{0.3+0.59D/K} \quad \text{for } D/K > 1 \quad (20)$$

The  $D/K > 1$  situation is needless to say, the practical case for rubble mound breakwaters.

Fig. 40 is a diagram showing the relation between  $\operatorname{tg} \phi$  and  $D/K$  with special reference to the W-ratios in practical rubble mounds. Table 7 corresponds to Table 6, referring to spheres only. From this table it may be noted that the figures indicated in column 3 are about 0.1 lower than the figures in column 2. The maximum difference in friction angle is, however, only approximately 5 degrees.

TABLE 7 POPULAR WEIGHT RATIOS IN RUBBLE MOUNDS AND THE CORRESPONDING RATIOS BETWEEN DIAMETERS IN ARMOR AND SUBLAYER,  $\phi$ 'S FOR SPHERES ACCORDING TO FIG. 37 AND TO FIG. 40

Weight ratios	$\operatorname{tg} \phi$ (Fig. 37)		$\operatorname{tg} \phi$ (Fig. 40)	
W to W	1.2	(50°)	1.1	(48°)
W to W/2	1.05	(47°)	0.95	(43°)
W to W/10	0.85	(40°)	0.7	(35°)
W to W/20	0.7	(36°)	0.6	(31°)
W/2 to W/10	0.9	(38°)	0.8	(39°)
W/2 to W/20	0.85	(40°)	0.7	(35°)

The improvement of slope stability against sliding by the use of W/10 instead of W/20 as sublayer, is  $0.7/0.6 \sim 1.15$ . The improvement of the stability by the use of a W/2 layer between the W and the W/10 layer, is  $0.8/0.7 \sim 1.15$  or figures very similar to these valid for the quartzite grains (blocks). This situation should be kept in mind whenever sliding is assumed to become the major danger to stability.

Other interesting details should be noted. In ref. (25) the U.S. Army Corps of Engineers warns against the use of only one layer of armor blocks because this lowers the safety factor and increases the risk of collapse of the entire design by

removal of the armor layer. From Table 7 it may be noted that  $\text{tg}\phi$  for  $W/W$  (two layers of weight  $W$ ), is 1.1 (3rd column of Table 7) while for  $W/\frac{W}{10}$  it is 0.7 only. It has occasionally been recommended to place a  $W/2$  layer between the  $W$  and the  $W/10$  layer. The advantage of this is obvious from Table 7. The  $W/\frac{W}{2}$  is 0.95 and the  $\frac{W}{2}/\frac{W}{10}$  ratio is 0.8 compared to 0.7 for the  $W/\frac{W}{10}$  ratio. The question, however, is whether one can compare the following two conditions directly;

- a) dry condition where failure is caused by sliding which means that the stability =  $f$  (angle of repose), and
- b) wet condition under wave action where failure is mostly caused by lift and/or overturning forces. "Toesliding" does not occur until higher damage ratios are reached.

Looking at the results of test-series 12 (Fig. 41) a comparison between the angle of repose (dry conditions) from Table 4 and the damage diagram from the previously mentioned stability tests with quarry stones as cover layer (Fig. 41), reveals the importance of friction between armor and sublayer for the stability of a quarry stone breakwater. This may be noted from the fact that the stability is higher when a linen cloth is put in between armor and filter than it is for the common rubble mound (curve 2). It may be noted that the internal forces are of limited order when the lower end of the impervious layer is kept above a certain elevation (curve 1, 2, 3). The increased stability in case of wave attack (curves 3 - 2 - 1 in Fig. 41) therefore seems to be related to the higher angle of repose (increased "friction").

In case of a cover layer of spheres (Fig. 42) one could, however, expect that model effects would be more pronounced, which means that the angle of repose for spheres decreases with increasing unevenness of sublayer. This seems, however, not to be the case. A more uneven sublayer increases the unevenness of the cover layer ( $d\phi$  increases), but simultaneously contact pressure in the armor layer is reduced ( $N$  decreases). Table 8 compares the wave height causing failure in case of an armor layer consisting of spheres and the angle of repose for a sheet of quarry stones placed on the same sublayer. A remarkable increase in stability with increasing unevenness is

noted just as for the quarry stone tests in Fig. 41. The stability in case of wave action therefore seems to increase with increasing angle of repose ( $\phi$ ) for dry conditions. That  $\phi$  increases with increasing unevenness, even for spheres, may be explained as follows:  $\phi$  is a function of the contact pressure between the spheres ( $N$ , Fig. 42) and the angle between the force direction and the slope ( $\Delta\phi$ ).  $\phi$  therefore may be expressed statistically as follows,  $\phi = f(\Delta N_n)$ , where  $\Delta N_n = \Delta\phi_n \cdot N_n$  and  $N_n = f(\sum_1^n G \cos\alpha, 1/\Delta\phi_n)$ .  $n = 1, 2, \dots, m$ , where  $m$  is total number of spheres on the slope.

The conclusion is that for dry conditions the angle of repose for quarry stones as well as for spheres as cover layer increases with increasing unevenness of the sublayer. The stability in case of wave attack seems to increase with increasing angle of repose for dry conditions.

TABLE 8	Failure wave height for spheres	Angle of repose for quarry stone
Perforated steel plate	$H_f = 9.0 \text{ cm}$	$\phi = 35.2^\circ$
Plastic sheet	$H_f = 9.5 \text{ cm}$	$\phi = 43.6^\circ$
Directly on the subl.	$H_f = 10.0 \text{ cm}$	$\phi = 59.5^\circ$

Note: The wave height causing failure seems to increase with increasing angle of repose.

#### SLOPE GEOMETRY

The above mentioned analysis of the stability of spheres refer to an ideal geometry and the results should as mentioned above be interpreted accordingly as a "trend". It is obvious, however, that the slope angle and the roughness are important parameters. The "squeezing power" increases with the slope angle and roughness increases stability and decreases the number of blocks needed to provide enough squeezing power to secure stability of the block layer in general. The requirement to increase of slope angle, however, is contradictory to the requirement of general stability of the armor layer against hydraulic lift forces which calls for a small slope angle.

It should be noted, however, that the two kinds of analyses differ in this respect that the mathematical model assumes a "wet condition" under wave action, the other a "dry condition". The requirements which refer to the former carry most weight as the flat slope definitely is the most stable, particularly if its members have a rough surface providing maximum of friction in all directions. This, however, does not eliminate the importance of the squeezing forces which may be increased by increase of "the number of blocks". Combining these requirements one arrives at a gentle "wide" slope or - by practical interpretation - to a slope which is gentle and wide in its most exposed section. Geometrically speaking this means an S-shaped profile with the flat part placed close to but above sea level.

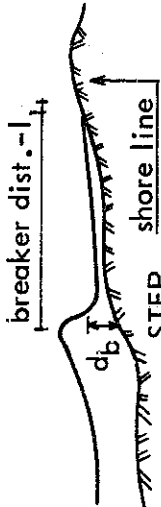
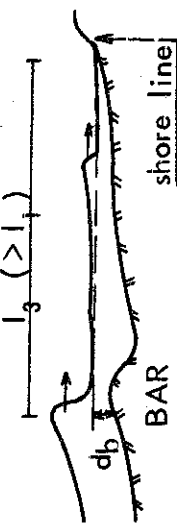
As mentioned in the following paragraph it is a known fact that such "berm-profiles" particularly if blocks are placed with the longest side pointing downward are the most stable and often are developed by nature itself which does not necessarily mean that they should be "designed by nature". It will in this respect be interesting to take a look at the so-called "selfadjusted profiles", starting with the geometry of natural beaches.

#### SELFADJUSTED PROFILES (12)

a - Relation between wave action and beach profile characteristics. Kemp (26) found that the ratio of the duration of uprush of a wave,  $t_a$ , to the wave period,  $T$ , characterizes flow conditions on a beach. The phase difference defined as  $t_a/T$  thus enables wave and beach conditions to be classified as "surge", "transition" or "surf" condition each with its own characteristic flow pattern. The corresponding equilibrium profiles are shown in Table 9. This classification was based on the observation that for low phase differences the broken wave was able to surge up the beach to the limit of uprush, and return as backwash to the breaker point before the succeeding wave broke. The flow shoreward of the breakers was distinctly oscillatory, and the beaches steep and plane. As the height of the incident wave increases further, the crest height ceases to increase and later begins to diminish.

TABLE 9.

## SHORT TERM VARIATION BEACHES - "EQUILIBRIUM PROFILE"

Surge conditions	Transition conditions	Surf conditions
	Beach cups are developed by the three dimensional flow pattern	
Summer - shingle beaches  $H_o/L_o < 0.02 - 0.03$	Unstable transition zone for the phase difference ratio $\approx 0.02 - 0.03$	Winter, storm - sand beaches  $H_o/L > 0.02 - 0.03$
SURGE      The transition from step to bar type profile is fully achieved once surf conditions are established Thus $H_b$ critical (step-bar) is a function of the wave period, ) : $H_b(Cr) \sim T$		
Beach profile dim. vs. wave characteristic $1 \sim \sqrt{H_b}$	$1 = K \cdot H_b \cdot \sqrt{H_b/D}$	$1 = K \cdot H_b \cdot \sqrt{H_b/D}$
$H_b \sim D \sqrt{\cot \alpha}$ where $\alpha$ is the beach slope.		

With the retreat of the beach crest and the seaward movement of the break-point ( $l_b$  increases) the uprush time increases. As a result the backwash is not completed before the next wave breaks. This condition involves interference between the backwash of one wave and the uprush of the next, and the oscillatory nature of the flow gave way to a transition flow regime with some increase in the interchange of water between the zones landward and seaward of the breakers.

As the phase difference increased further to values greater than unity, the transition phase gave way to "flow" conditions in which successive breakers continually spilled water into the inshore zone, producing a corresponding return-flow. In accordance with this change in wave conditions, the step profile gradually becomes infinite and finally changes to a bar profile. After the bar profile has developed in full, the breakers become less violent, since the momentum effect of backwash is reduced.

The importance of the phase difference on run up and therefore on the stability of a rubble mound breakwater will not be discussed further in this paper. Research on this topic is presently in progress as described later and will result in a M.S. (Ph.D.) thesis on the subject.

b - Selfadjusted stable breakwater slope. The development of a stable breakwater profile under wave action shows similar characteristics. Due to the steep slope and coarse material "erosion" takes place on the upper part of the slope and accumulation of the "eroded material" takes place in the lower part.

The need for better reasoned design procedures resulting in greater degree of compatibility between wave attack and cross sectional profile of rubble mound breakwaters, is pointed out in ref. (31). This again opens the possibility for use of smaller stones. Fig. 43 shows a self-formed, stabilized rubble mound breakwater as described in (31). The curve-lined profile may be simplified by the three straight dotted lines, AB, BC, CD.

Similar tests were run by Popov (30) who sought information about stable profiles of earth dams in reservoirs. Fig. 44 shows a typical "abrasion profile" (30). The stable slopes have the following four characteristic zones (the heavy line 1-2-3-4-5). Zone 1-2 from maximum uprush down to the S.W.L.-line corresponds to curve A-B on the breakwater slope. Below comes a flat underwater zone (2-3 corresponding to B-C). Next comes the underwater roller zone 3-4. Below follows the accumulation-zone (4-5 corresponding to CD).

The similarity of the step profile (Fig. 45 a), the self-adjusted breakwater profile and the dam profiles (Figs. 43 and 44) is apparent. All profiles consist of a flat zone above and below S.W.L., which form a "false" beach. Above and below this zone follow about equally steep "underwater" and "uprush" zones. It is furthermore known that the distortion of the selfadjusted profiles  $\Omega = \mu/\lambda$ , where  $\mu$  = vertical scale ratio and  $\lambda$  = horizontal scale ratio, decreases with decreasing size of the material forming the beach (the beach flattens). Coastal movable bed scale model relationships have been analyzed by Watts (32) and by Noda (29). Model laws, however, only apply within certain ranges of the size of the beach material (approx. 0.1-0.5 mm in diameter). They can therefore hardly be used with material of 0.6-60 mm in characteristic diameters. However, to emphasize the similarity in different beach profiles formed by waves, the step profile in Fig. 45 a, a profile shown in Fig. 46 a taken from Watts (Fig. 5 in (32)), and the dam profile in Fig. 44, have been modified to match the breakwater profile in Fig. 43. This was done by multiplying the vertical and the horizontal scales by a certain number and resulted in Figs. 47 a and 47 b. Considering the breakwater profile (Fig. 43) and the step profiles (Figs. 45 a and 46 a) as "prototypes" (p) and using the same procedure results in the transformed profiles shown in Figs. 45 b and 46 b). The combined results of plotting the profiles using a certain distortion factor are tabulated in Table 10. It is seen that the distortion as expected decreases considerably with decreasing grain size diameter-ratio ( $n_D = D_m/D_p$ ).

TABLE 10	Grain size D in mm	Grain size ratio $n_D$	Horizontal scale ratio $\lambda$	Vertical scale ratio $\mu$	Distortion $\Omega = \mu/\lambda$
Rubble mound breakwater	313	1	1	1	1
Dam (Fig. 47a+b)	0.6	0.2	4.92	3.3	0.66
Beach profile from Watts (Fig. 46 a+b)	0.22	1/141	11.5	1.38	0.12
Step profile (Fig. 45 a+b)	0.1	1/313	2.5	1	0.4

Noda (29) found the following relation between  $n_{Y1}$ ,  $\lambda$ ,  $\mu$  and  $n_D$  ( $n_{Y1} = (\gamma_s - \gamma_f)/\gamma_f$  is the relative specific weight) for variation of grain size between 0.1-0.5 mm:

$$n_D \cdot n_{Y1}^{1.46} = \mu^{0.55} \quad (19)$$

$$\lambda = \mu^{1.32} \cdot n_{Y1}^{-0.35} \quad (20)$$

In this case  $n_{Y1} = 1$  which reduces Eqs. 19 and 20 to  $n_D = \mu^{0.55}$  and  $\lambda = \mu^{1.32}$ . This relationship, however, does not fit the data in Table 10, except for the distortion ratio between the dam profile and the breakwater. Eq. 20 gives  $\lambda = \mu^{1.32} = 3.3^{1.32} = 4.8$  which is approx. the ratio found by the plotting method. The  $n_D = f(\mu, \lambda)$  relationships by Noda (29), however, do not apply in this case. This is indeed to be expected, because the destructive forces in case of gravel or rock fill cover material are different from those in case of a beach of fine sand. More data are needed to develop well defined model laws which apply for beach material from fine sand to gravel.

For design of breakwaters or any protecting coastal structure, it is important to note the general similarity between profiles formed by waves. A profile may be schematized by dividing it into three zones as discussed above. It is obvious, however, that the hitherto commonly used trapezoidal linear slope profile, causes a very uneven distribution of forces by waves adverse to stability and in hydraulic sense is not very practical.



## DISCUSSION, PART I AND PART II

The results of the analyses, hydraulic and mathematical model tests mentioned in Part II may be summarized as follows: It is important to secure adequate friction between armor units and the sublayer to avoid sliding down of units. Friction between units is equally important because it decreases the possibility of these units to jumping out of the mound. Friction forces between cover units and sublayer increase with the grain size of sublayer due to increasing interlocking and decreasing "bridging" armor units. This compares well with the experience that large flat pieces of armor units which would also be exposed to large lifting forces by uprush and downrush should be avoided. U.S. Army Corps of Engineers standards in fact take this condition to consideration as is indicated by the requirements for ratio of size between armor and sublayers. Forces between single armor units are obviously mobilized best when these units are placed with the long side perpendicular to the slope (27). This in turn requires a rather even placement to ensure that blocks which are not flush with the surface of the mound are not exposed to inertia and drag forces by downrush causing large overturning moments. Placement should needless to say be careful so that blocks support each other instead of being separated from their neighbors thus increasing the possibility of units jumping out due to lack of squeezing forces by other units. The importance of slope geometry in relation hereto is mentioned below.

The discussion and conclusion of Part I of this paper emphasized the importance of avoiding high downrush forces in the slope particularly where "resonance" between uprush/downrush period (downrush in lowest position at toe of breaking waves) and wave period may occur and the importance of taking measures against combinations of hydrostatic uplift pressures and lift forces by downrush and toe velocity in that particular area. The importance of this "resonance phenomenon" is obvious from tests undertaken recently. A comprehensive report on this subject by stud.lich.techn. Ali Riza Gunbak is forthcoming. The results emphasizes that the presently used design formulas for

rubble mounds which neglect the wave period are inadequate and under certain circumstances give very unsafe results.

#### PRACTICAL DESIGN PRINCIPLES CONCLUSION, PART I AND II

Due to the above mentioned results and experiences it seems practical to divide the rubble mound slope for design and construction into three zones, each with its characteristic block properties (Fig. 48). The "platform" BC, has a relatively gentle slope e.g. 1 in 3. Waves plunge at point C. Run-up is reduced by turbulence and energy absorbtion due to the phase difference between uprush and downrush. The breaking wave usually does not strike the exposed breakwater slopes, but plunges into a "stilling basin" on the gentle part of the breakwater. The steep slope, CD, separates backwash from the retreating velocity field in the downrush at the toe of the breaking waves, and therefore makes the backwash incipient breaker interaction less violent. This reduces the maximum normal and parallel forces at the lowest level of wave retreat - and these forces are usually most critical for the stability of a breakwater. Furthermore, a layer HG with low permeability prevents outflow from being concentrated at the breaking point where the external forces primarily suction in the toe of the breaking wave are maximized.

Another layer, FE, with lower permeability, prevents inflow above point E, which reduces the build up of hydrostatic pressure in the mound during wave retreat.

In zone BC the drag coefficient of the blocks parallel to the slope and the exposed area of armor blocks should be minimized. In zone CD the drag coefficient of the armor blocks perpendicular to the slope should be minimized due to the high normal forces and the concentrated outflow. The upper slope AB may be relatively rough as it is not exposed to high velocities. Roughness decreases uprush and lower downrush velocities. Both are advantageous.

The importance of layer HG is obvious from the tests mentioned in Part I as well as from preliminary tests with such layer placed in the mound. In order to quantify results - instead of using the popular procedure of just "counting blocks" which left the mound, a very questionable and superficial procedure - an instrument has been developed, called the "Optical Break Down Sensor" which allows quantification. The main principle of this device is that photographic reproduction keeps memory of the original situation. Deviations appear with great contrast.

The basic principle is called "solarization" or "bas-relief" effect in photography. It is based on the "trick" of applying a negative film to mask out all highlights passing through a positive film. By complete alignment of the positive and negative a gray picture results with no details. Slight misalignment lets the details appear again, lighter or darker. This principle can be modified to suit the needs of an OBD-sensor. Direct reversed, image in the camera is used instead of a positive film.

The practical procedure in sensing of the onset of structural changes (start of breakdown) is that a negative of normal gamma (contrast) is slightly underexposed or overexposed and used as a mask in the camera. It is accurately aligned to show minimum light transmission as measured by a photocell.

Changes from the original cause an output from the photocell. This output is a function of changes in the motive. This output can be recorded as an analog value on stripchart recorder or digitized by an analog/digital converter for further processing.

This instrument will first be calibrated and used in the laboratory next used to check the stability of breakwaters in Northern Norway in a cooperative effort with The Norwegian Board of Maritime Works which has comprehensive experiences on breakwater design and maintenance problems.

The optimal elevation of the berm depends upon the combined effect of tides and waves. Tidal ranges vary. On the open

deep water, sea coast tides are identical with "astronomic tides". Wave action, however, is independent of tidal range but may be a little more severe at high tide than at low tide. The most economic design of the berm, needless to say, is associated with the lowest tidal range. If tidal range is high, the berm has to be wider. One may say that the berm may be allowed to be less effective during normal tide and wave conditions. Design procedure in such cases, therefore, becomes an optimization of action and reaction considering probabilities of combined tide and wave action and the corresponding expected damage. This will result in an economic width of berm at the elevation where it does most good - but it may also - e.g. in the case of a large tidal range - result in omission of the berm because it becomes too wide to justify it.

It has been known for a long time that rubble mound structures when damaged or - more politely expressed - when "maturing" may develop an S-shape. The new breakwater at Mangalore, India, on the Arabian Sea, was built with an S-shape to avoid heavy handling equipment. Fig. 49 (The Dock and Harbour Authority, No. 633, July 1973) shows breakwaters at Plymouth, England and Cherbourg, France, built 150-200 years ago. Similar experiences when the sea was allowed to engrave its own profile in the mound are available at many places in Iceland and in Norway. This does not mean that structures should be built for nature's "maturing process" but that they should be designed as "cured" from the beginning.

The results mentioned are independent of the water depth in front of the structure but depend upon the wave spectrum and the possibilities included in the said spectrum for occurrence of the most critical situations with respect to stability. This refers to the violence of the downrush as well as to the possibilities of resonance as defined and the occurrence of a sequera of waves near the critical resonance period.

Details of design may at this stage best be determined by hydraulic model experiments with irregular waves utilizing

the basic principles on separation of water flows mentioned above in conjunction with geometrical features. They will also determine optimal berm elevation and (economical) width, and the best location of the two impermeable layers, FE and HG.

The practical aspects of placing the sheets have been discussed with contractors. They see no problems of placing the upper sheet which could be thick nylon or of making the S-shape in the prescribed manner. The lower sheet could, however, involve some difficulties, particularly on exposed shores. In such cases injection of cement mortar or asphalt mortar would replace the sheet and this would decrease the difficulties. Preference is given to hot asphalt mastix with reference to experiences in Holland, England and Denmark. Another conclusion of the research is that the existing empirical design formulas are inadequate and often unsafe because they ignore the importance of wave period.

This points out the necessity of designing rubble mound structures or any other sloping permeable structure based on design criteria which describe the actual events in nature accurately. It is not enough to select a "design wave" and a "proper"  $K_A$ -value based on laboratory experiments. It is not either enough to select a "design storm" or a specific "design spectrum". The design wave or the design spectrum gives a "load" which is sometimes regarded as the maximum exposure which can occur. This could be far from the truth, however. A much more reliable and scientifically as well as practically better reasoned design procedure is first to select one from a technical as well as economical view particular attractive design with alternatives. Next to examine a number of actual wave spectra from the site under consideration including analyses of extreme and trains of approximately regular waves with special reference to the correlation between succeeding waves as described

in papers in print by O.G. Houmb and H. Rye "Analysis of Wave Data from the Norwegian Continental Shelf", Proc. 2nd International Conference on Port and Ocean Engineering under Arctic Conditions, Reykjavik, Iceland, 1973 and "Wave Group Formation among Storm Waves", Proc. 14th International Conference on Coastal Engineering, Copenhagen, 1974, by H. Rye.

Results of experiments of earlier date on stability versus uprush - downrush - resonance and hydrostatic pressures will then be of guidance with respect to a refinement of structural details in each particular case using the design principles mentioned above and tests which concentrate on combinations of certain waves and periods which occur in the actual spectra. Particular reference should still be paid to conditions which produce the most dangerous resonance phenomena. Such conditions may occur during a number of storms and the most dangerous of these is not necessarily associated with the highest waves, uprush/downrush or downrush. It could be connected with the succession of a number of waves causing repeated resonance.

This is not a "philisophy" but the result of a great number of actual observations in the North and Arctic seas where a highly professional experience is available - but unfortunately unknown. The above changes conventional design procedures to wave probability analyses in relation to structural hydraulic, up and downrush and wave breaking characteristics and introduces in fact practices similar to those which are common in soil mechanics as well as other structural resonance and "vibration" analyses as well as in hydraulic design considering eddy resonance (Strouhal number) and wave mechanics analyses of shock or stagnacy pressures versus eigenperiods of vertical breakwater structures.

## REFERENCES

23. Bjerrum, L., "Subaqueous Slope Failures in Norwegian Fjords". Proceedings, the First International Conference on Port and Ocean Engineering under Arctic Conditions, the Norwegian Institute of Technology, Trondheim, Norway, 1971.
24. Day, Y.B. and Kamel, A.M., "Scale Effect tests for Rubble Mound Breakwaters". Research Report H-69-2. December 1969, U.S. Army Engineer Waterways Experiment Station, Corps of Engineering, Vicksburg, Mississippi.
25. Jackson, R.A., "Design of Cover Layers for Rubble Mound Breakwaters Subjected to Nonbreaking Waves", Research Report No. 2-11, U.S. Army Engineering Waterways Experiment Station, Vicksburg, Mississippi, 1968.
26. Kemp, P.H., "The relationship between wave action and beach profile characteristics". Seventh Conference of Coastal Engineering, The Hague, Netherlands, August 1960, Vol. I.
27. Kidby, H. et al, "Placed-stone jetty, stone weight coefficients", Journal of Waterways, Harbor and Coastal Engineering Division, ASCE Vol. 90, No. WW4, Proc. Paper 4134, November 1964, pp.77-85.
28. Miller, R.L. and Byrne, R.J., "The Angle of Repose of a Single Grain on a fixed Rough Bed", Technical Report No. 4, Department of the Geophysical Sciences, the University of Chicago, May 1965.
29. Noda, E., "Coastal Movable-Bed Scale Relationship", Tetra Tech. Inc., Pasadena, California. See also Journal Waterways, Harbors and Coastal Division, ASCE, Vol. 98, No. WW4, Proc. Paper 9367, November 1972, pp. 511-528.
30. Popov, I.J., "Experimental Research in Formation by Waves of Stable Profiles of Upstream Faces of Earth Dams and Reservoir Shores". Seventh Conference of Coastal Engineering, The Hague, Netherlands, August 1960, Vol. 2.
31. Priest, M.S., Pugh, J.W. and Singh, R., "Seaward profile for rubble mound breakwaters". Proceedings Ninth Conference of Coastal Engineering, Lisbon, Portugal, June 1964, Chapter 35.
32. Watts, G.M., "Laboratory Study of Effects of Varying Wave Periods on Beach Profiles". Technical Memorandum No. 53, September 1964.

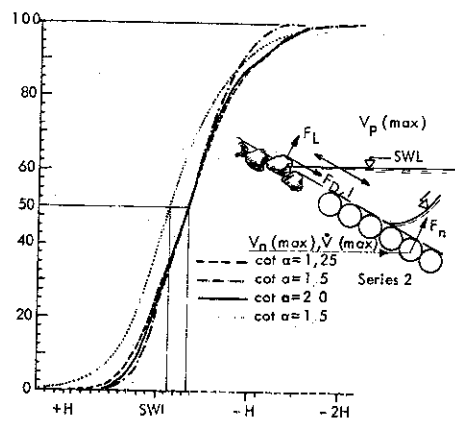


FIG. 1 - CUMULATIVE DISTRIBUTION OF DAMAGE ALONG THE BREAKWATER FACE (5) SERIES 1 AND 2

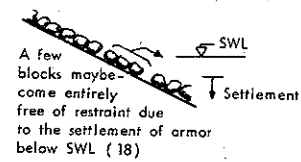


FIG. 2a - START OF FAILURE

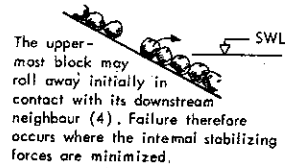
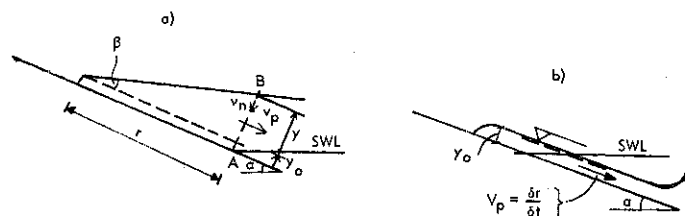
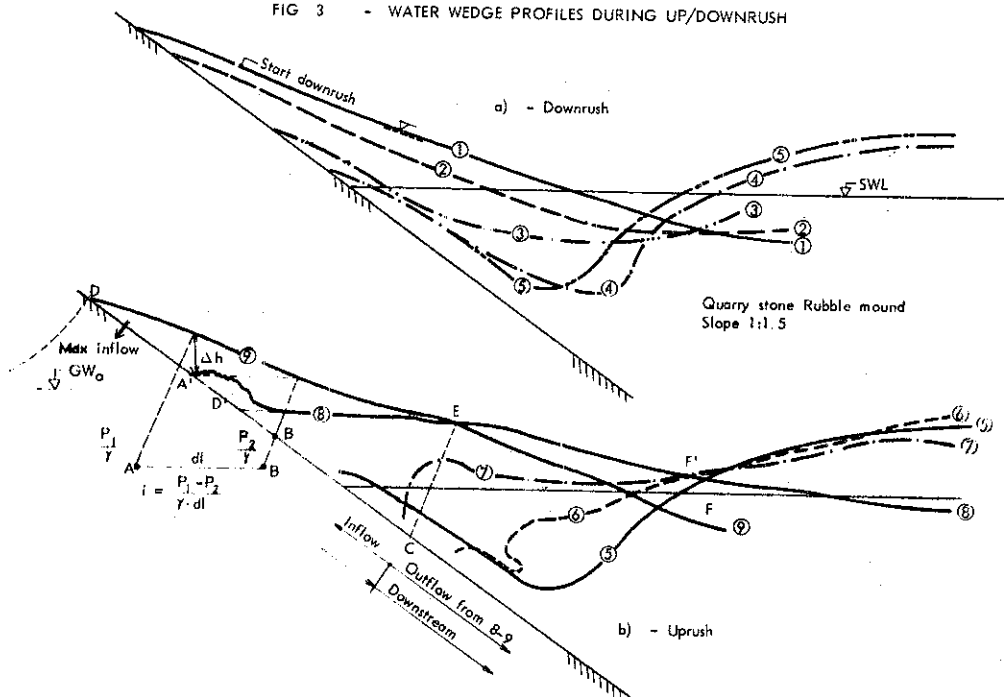


FIG. 2b - START OF FAILURE (5)

FIG. 3 - WATER WEDGE PROFILES DURING UP/DOWNRUSH



$$V_p = \frac{\partial r}{\partial t} + \frac{r^2}{y_o + r \tan \beta} \frac{1}{2 \cos^2 \beta} \frac{\partial \beta}{\partial t} = V_p(r) + V_p(\beta)$$

When  $\beta \rightarrow 0$  then  $y \rightarrow y_o$ ,  $\frac{\partial \beta}{\partial t} \rightarrow 0$ ,  $\rightarrow V_p(\beta) = 0$

$$\lim_{\beta \rightarrow 0} |V_p| = \frac{\partial r}{\partial t}$$

$$\frac{\partial \beta}{\partial t} \rightarrow 0$$

FIG. 4 - MODEL FOR COMPUTATION OF VELOCITIES AT SWL PARALLEL AND NORMAL TO THE SLOPE.



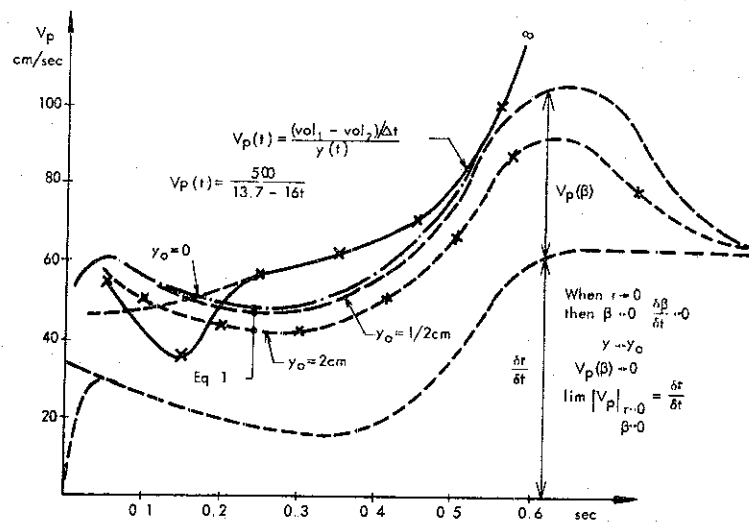


FIG. 6 -  $V_p$  AS A FUNCTION OF TIME DURING DOWNRUSH.

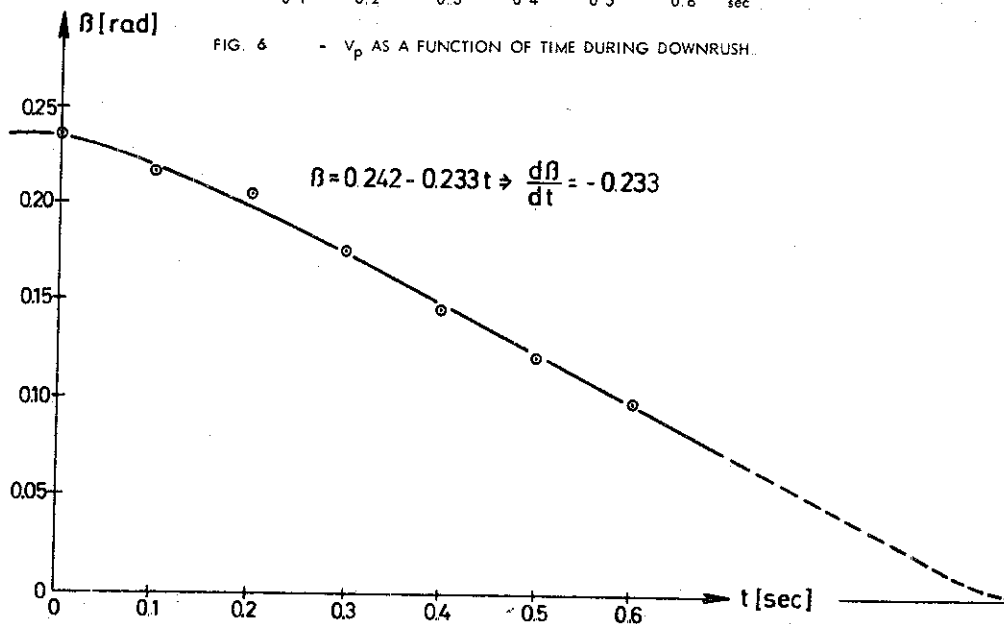


FIG. 5 -  $\beta$  AS A FUNCTION OF TIME DURING DOWNRUSH.

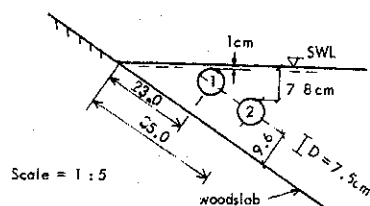


FIG. 7 - CROSS SECTION OF MODEL SHOWING LOCATION OF BALLS

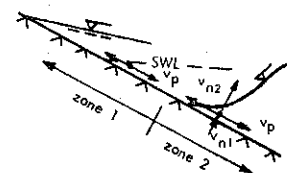


FIG. 9 - WAVE FORCE DISTRIBUTION ON A BREAKWATER SLOPE

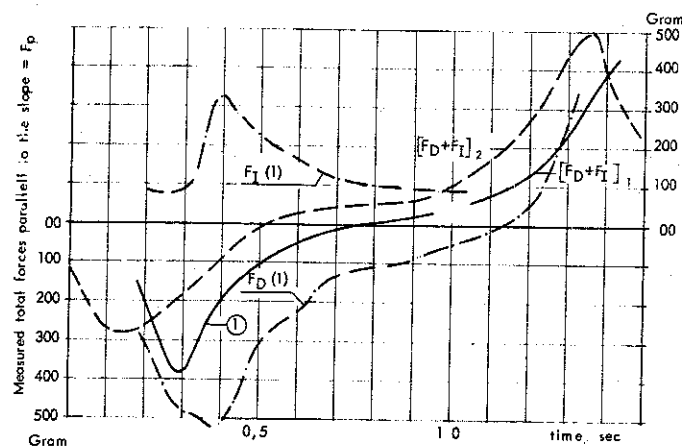
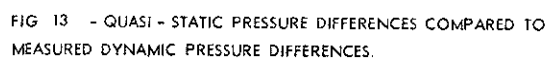
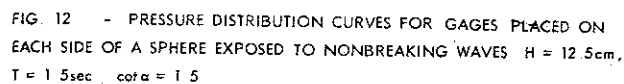
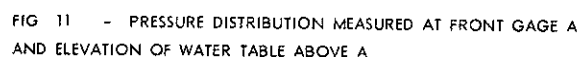


FIG. 8 - MEASURED FORCE DISTRIBUTION CURVES.



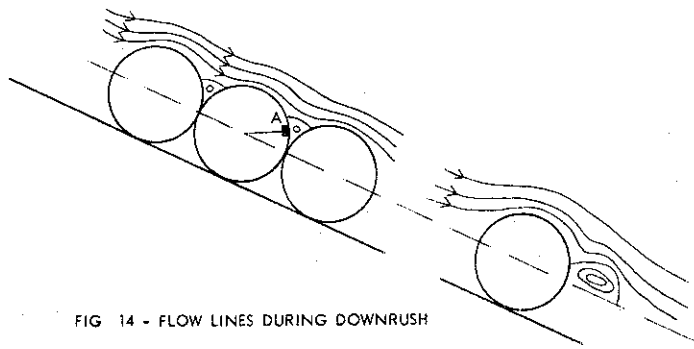


FIG 14 - FLOW LINES DURING DOWNRUSH

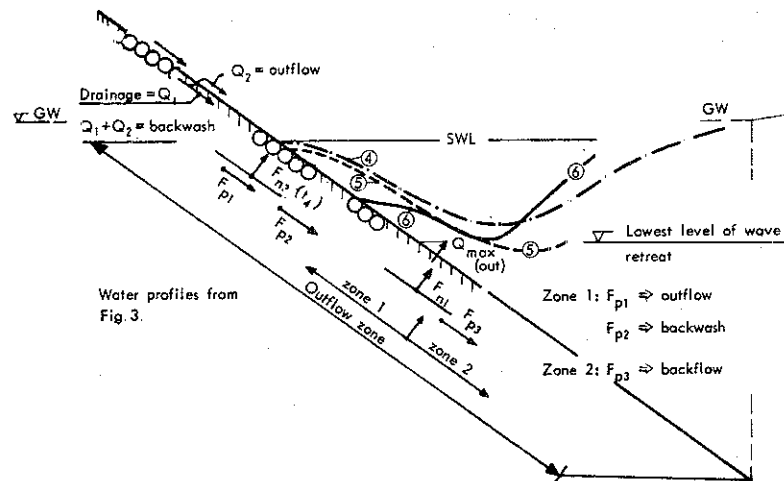


FIG 15 - WAVE PROFILES OUTFLOW CONDITIONS

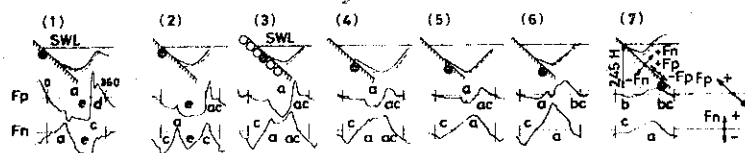


FIG 16 - TYPICAL FORCE DISTRIBUTION CURVES (28)

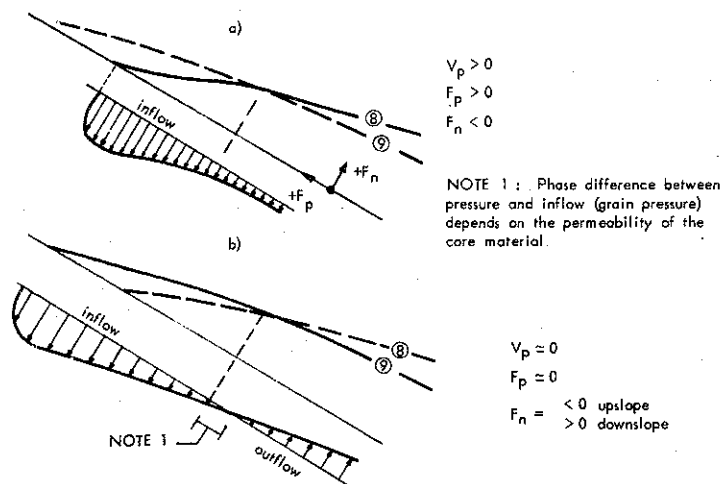


FIG 17 - INFLOW AND OUTFLOW FROM THE MOUND VERSUS WAVE PRESSURE

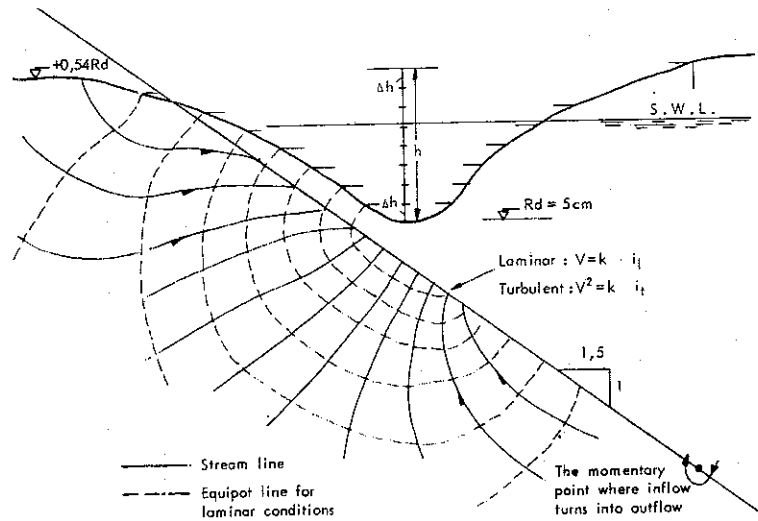


FIG 18 - FLOW NET IN CASE OF STATIONARY CONDITIONS AT MAXIMUM DOWNRUSH

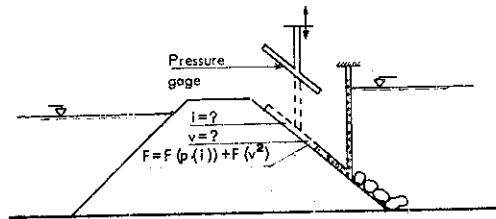


FIG 19 - MODEL TESTS FOR DETECTION OF FLOW GRADIENTS AND VELOCITIES

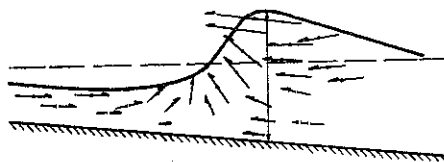


FIG 20a - VELOCITY FIELD IN A BREAKER

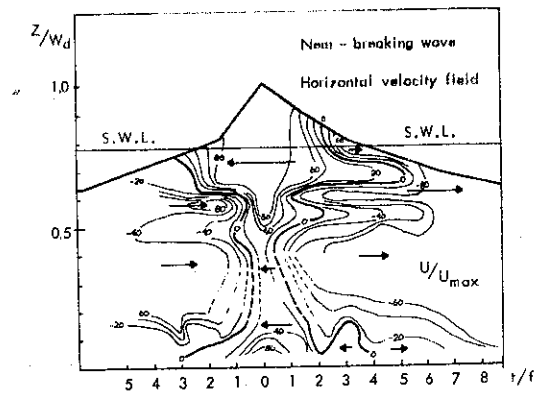


FIG 20b - WAVE PROFILE NEAR BREAKING AND RELATIVE VELOCITY FIELD (19)

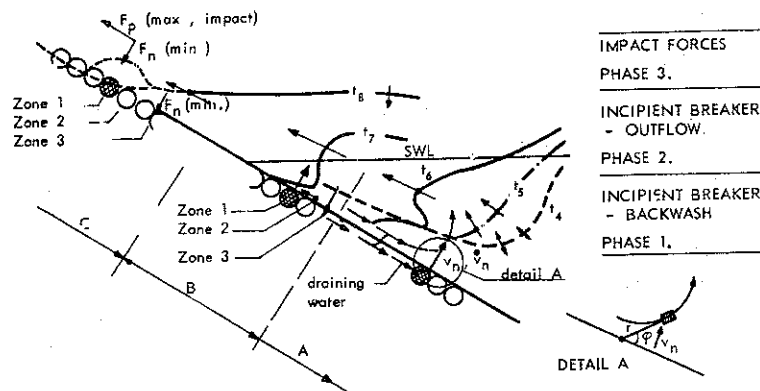


FIG 21 - FORCE DISTRIBUTION FOR PHASE 1, 2 AND 3

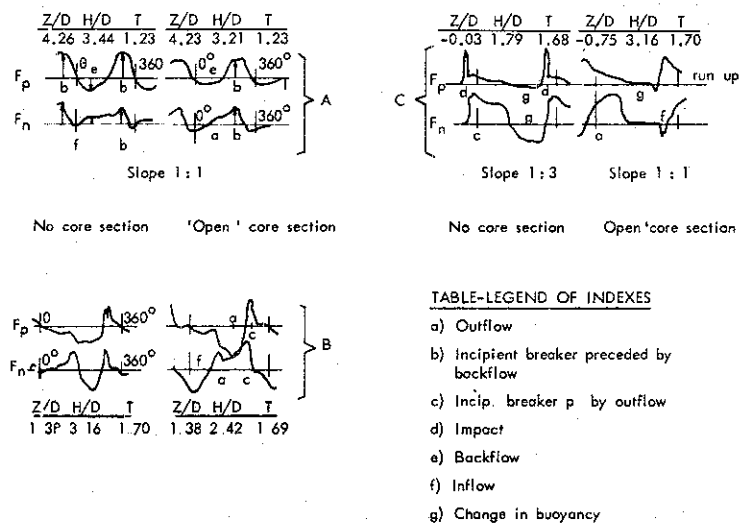


FIG. 22 - FORCE DISTRIBUTION CURVES FOR PHASE 1, 2 AND 3

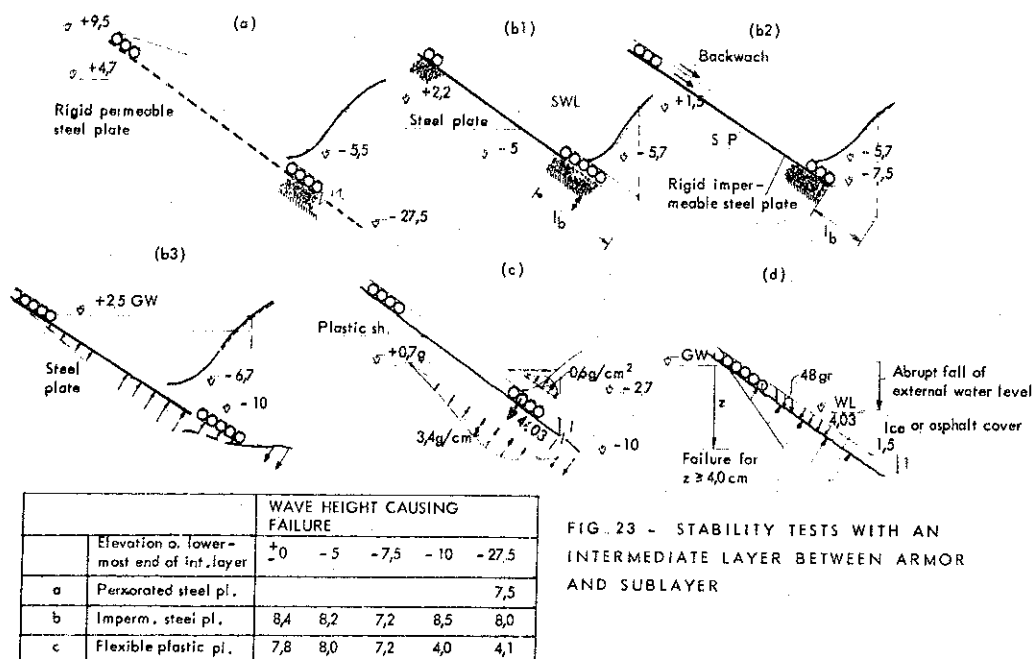


FIG. 23 - STABILITY TESTS WITH AN INTERMEDIATE LAYER BETWEEN ARMOR AND SUBLAYER

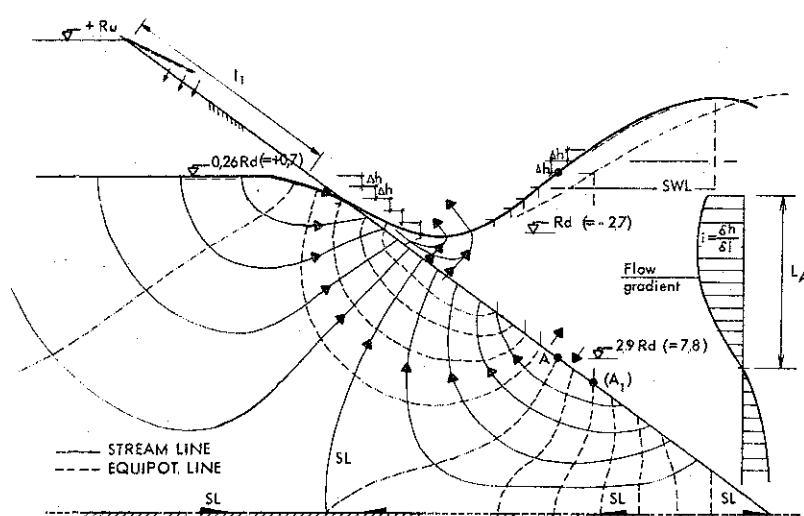


FIG. 24 - FLOW NET AND DISTRIBUTION OF OUTFLOW GRADIENTS FOR "STATIONARY CONDITIONS" AT MAXIMUM DOWNRUSH SLOPE 1:1.25. LOCATION OF POINT OF 'OUTFLOW - INFLOW'.

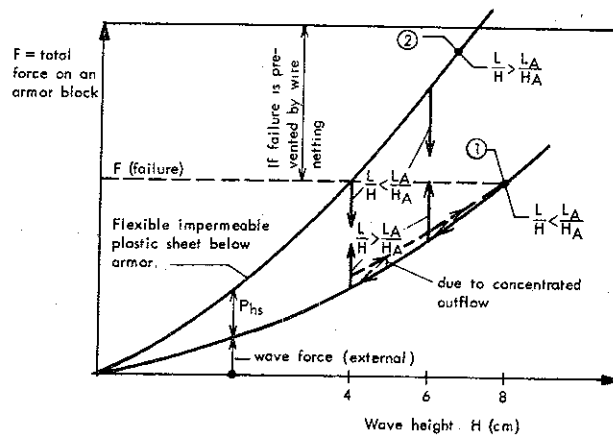


FIG. 25 - DISTRIBUTION OF FORCES CAUSING FAILURE AT MAXIMUM DOWNRUSH WITH AND WITHOUT AN INTERMEDIATE FLEXIBLE LAYER ( $\sigma_b = 0$ ) BETWEEN ARMOR AND SUBLAYER.  $L_A$  (See FIG 24.),  $H_A$  = WAVEHEIGHT CORRESPONDING TO  $L_A$

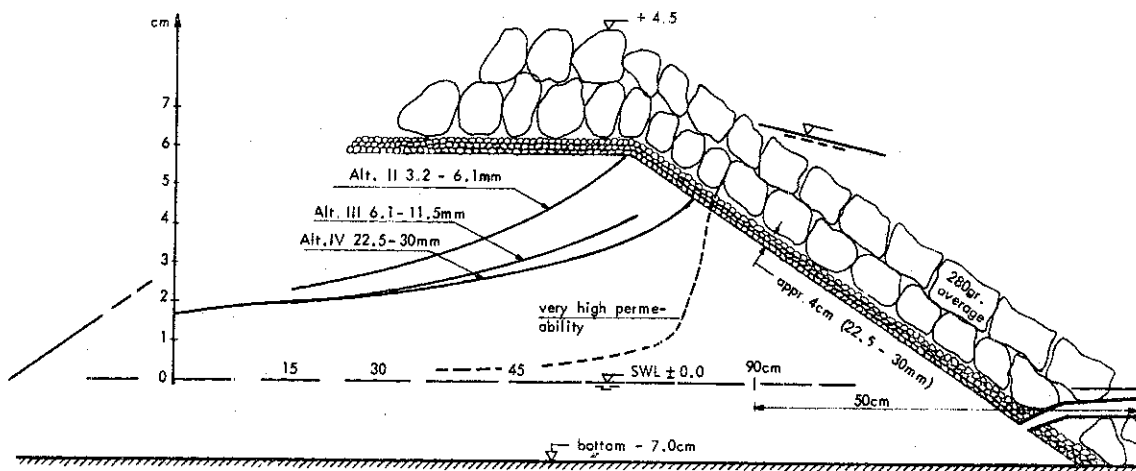


FIG. 26 - WATER ELEVATION IN THE CORE AT MAXIMUM UPRUSH FOR VARYING PERMEABILITY OF THE CORE

Note: Damage is more pronounced and occurs earlier for finer core material (alt. II) than with a more coarse core mainly for higher damage ratios.  $k$  = coefficient of permeability. Armor was 6 cm in diameter.

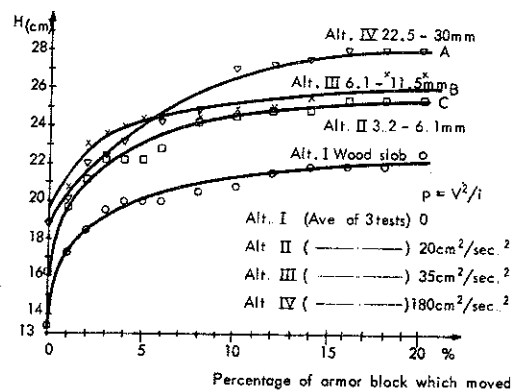
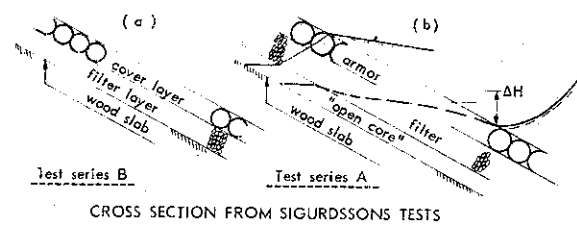


FIG. 27 - DAMAGE RATIO VS. WAVE HEIGHT FOR DIFFERENT CORE MATERIAL



CROSS SECTION FROM SIGURDSSON'S TESTS

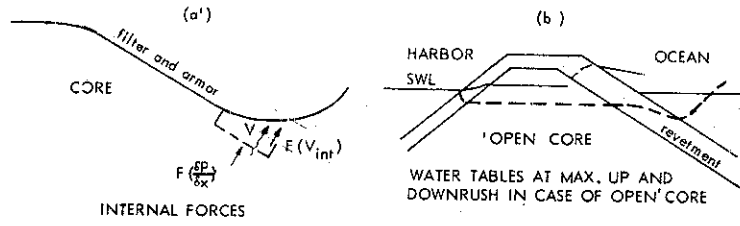


FIG 28 - THE IMPORTANCE OF THE PERMEABILITY OF THE CORE MATERIAL ON THE STABILITY CONDITIONS

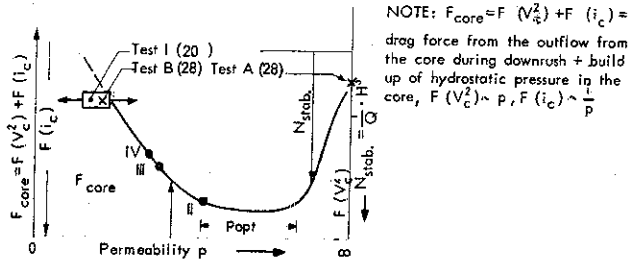


FIG 29 - PERMEABILITY OF CORE MATERIAL VS. BREAKWATER STABILITY

G = weight of sphere  
a = structure slope  
μ = coefficient of friction

Note: One horizontal row of spheres  
No 1 is affected by an external  
force ( $F_y$ ) or moment (M)

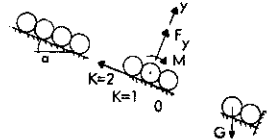
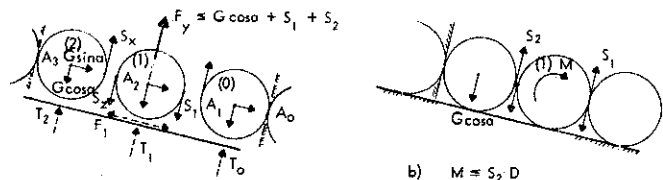


FIG 30 - DEFINITION OF SYMBOLS



At the moment of failure  $T_1 = T_2 = T_0 = 0$   
 $F_1 = F_2 = F_0 = 0$   
 $S_2 \rightarrow S_1$

Note: At the moment of failure the contact pressure between the affected sphere and the base becomes zero (statically determined system) which in turn means, (neglecting the dynamic effects), that  $S_1 = S_2$

FIG 31 - DEFINITION OF STABILIZING FORCES

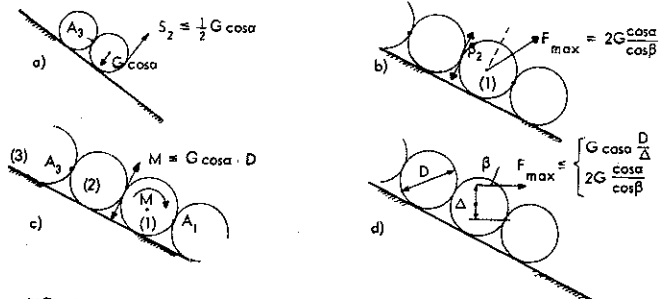
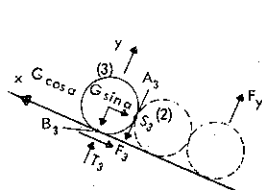


FIG 32 - MAXIMUM STABILIZING FORCES



Calculation of number of spheres above the affected sphere necessary to prevent sliding between the balls and between the balls and the base (admits full mobilization of the torque moment)

First calculate the slope angle (abscissa) and the coefficient of friction (y - ordinat) for stable condition for  $K = 3$  ( $F_3 = S_3$ )

FIG. 33 CALCULATION OF NUMBER OF SPHERES

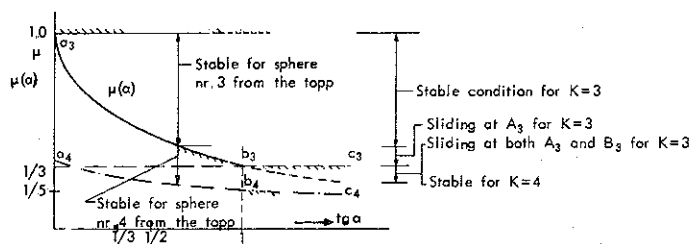
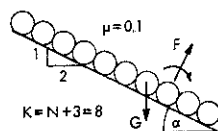
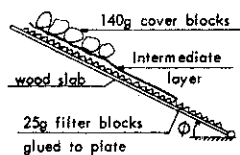


FIG. 34 - NUMBER OF BALLS NECESSARY TO STABILIZE THE TORQUE MOMENT VS. SLOPE CHARACTERISTICS



Consider as example  $\mu=0.1$ ,  $\cot \alpha=2$   
 $F_y$  increases and is maximized for ball No. 8,  $F=\text{const.}$  for  $K > 8$   
 $F_{3+N} = \frac{1}{2} G \cos \alpha \frac{1-(2N+1)\mu}{1-\mu(-1)^N}$

FIG. 35 - CALCULATION ON INTERNAL STABILITY



In test series (16) the angle of repose, for dry conditions, was found for different friction conditions (by means of an intermediate layer) between filter and armor layer. The results are shown in Table 4

FIG. 36 - CROSS SECTION OF MODEL,  $\phi_{\max}$  = ANGLE OF REPOSE

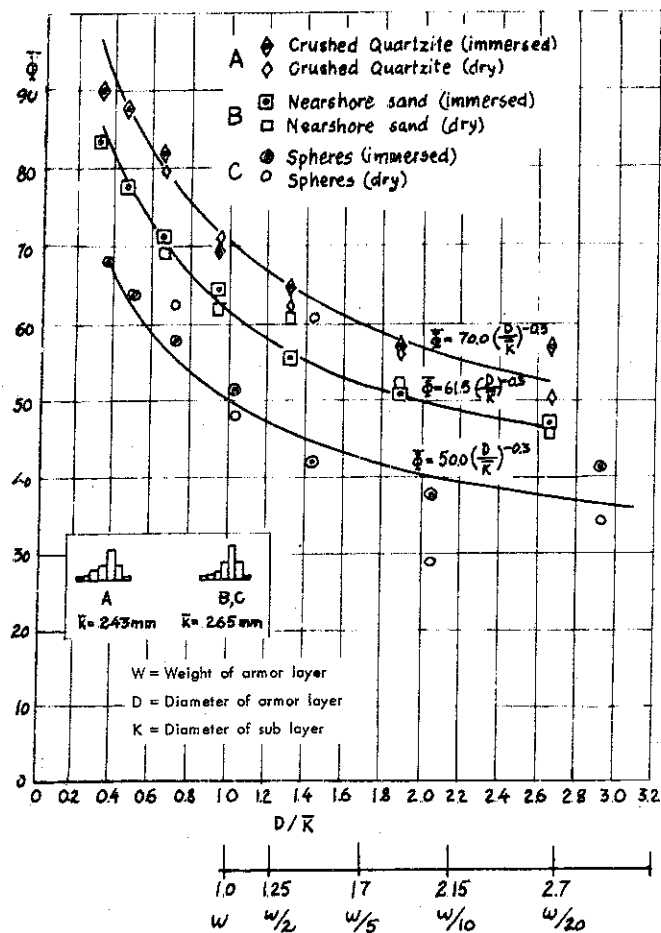
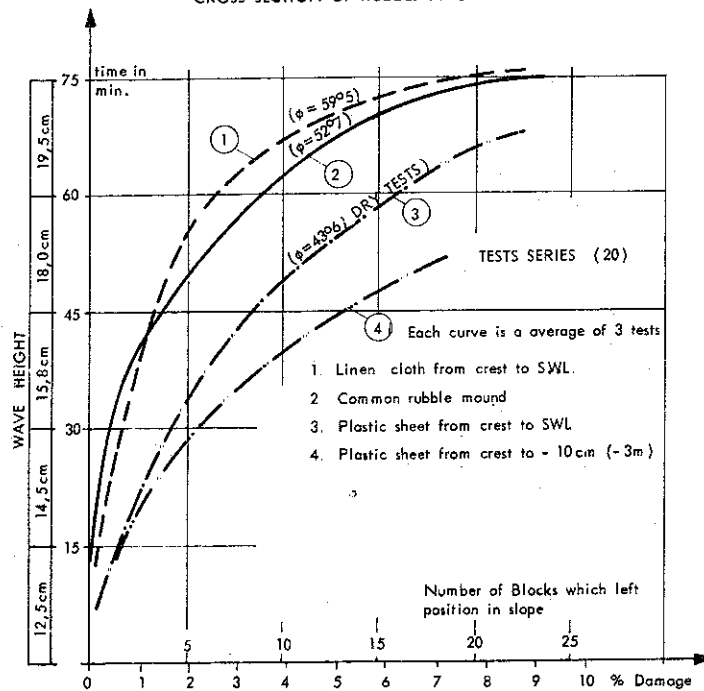
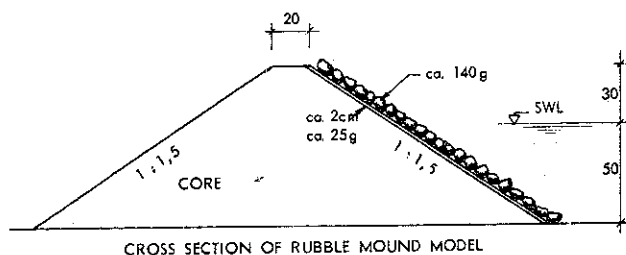
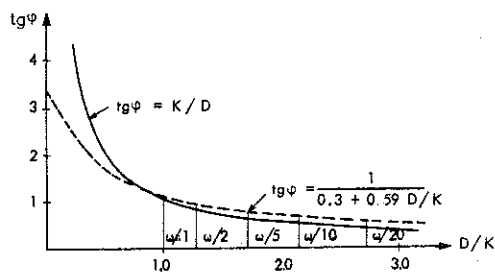
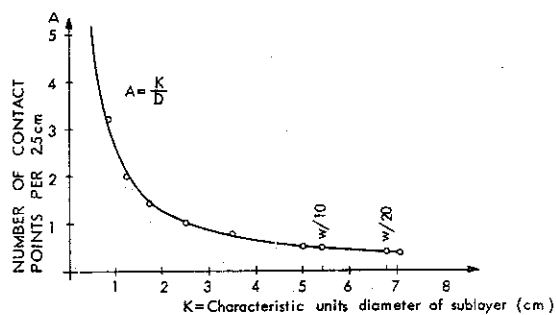
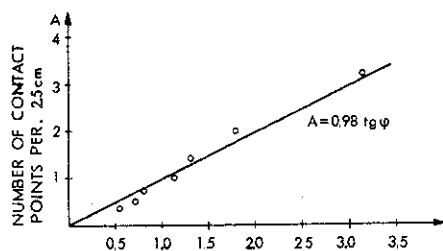


FIG. 37 -  $\phi$  AS FUNCTION OF THE D/K RATIO





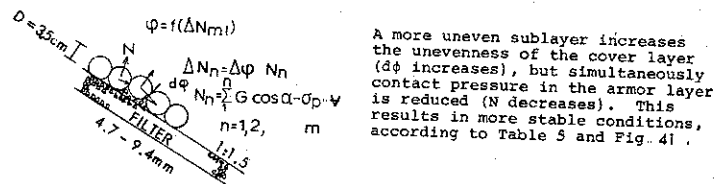


FIG. 42 - INFLUENCE OF UNEVENNESS OF ARMOR LAYER CONSISTING OF SPHERES ON THE ANGLE OF REPOSE.

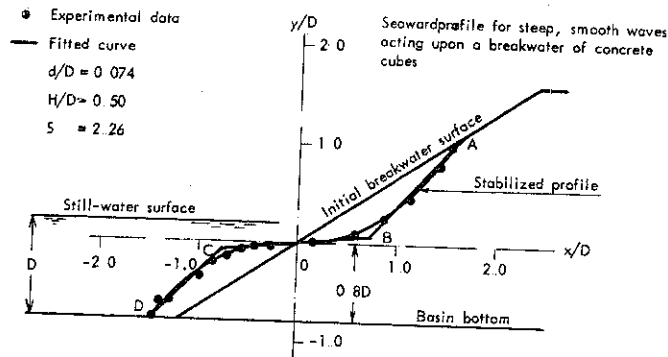


FIG. 43 - STABILIZED BREAKWATER PROFILE

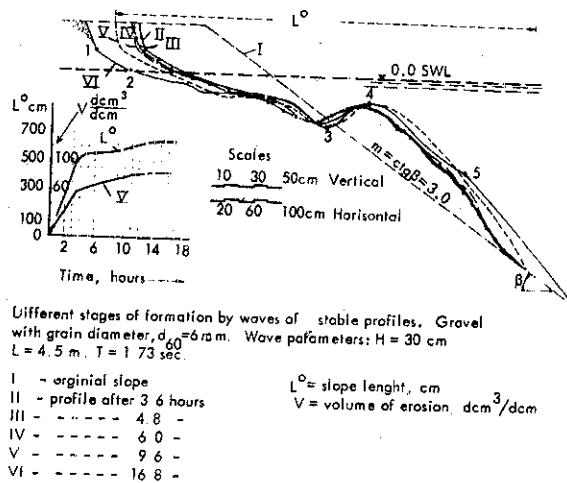


FIG. 44 - EXPERIMENTAL RESEARCH IN FORMATION BY WAVES OF STABLE PROFILES OF UPSTREAM FACES OF EARTH DAMS AND RESERVOIR SHORES

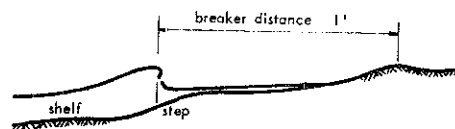


FIG. 45a - TYPICAL STEP PROFILE

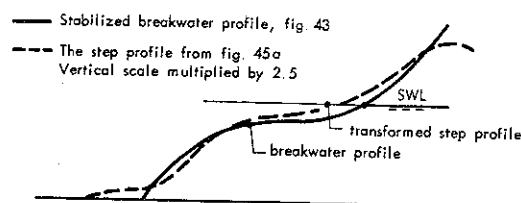
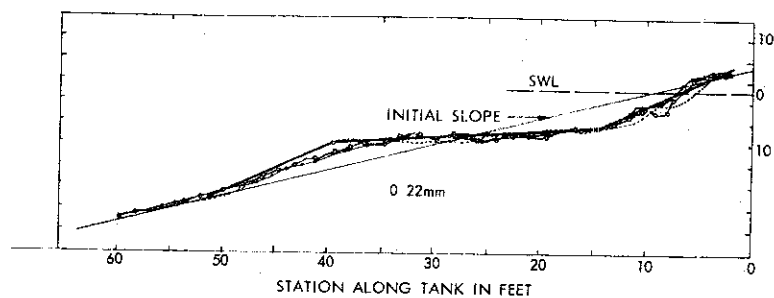


FIG. 45b - BREAKWATER PROFILE (FIG. 43) AND TRANSFORMED STEP PROFILE FROM FIG. 45a.



LEGEND  
 — Mean wave period 2 00 sec.  
 - - - Period varied  $\pm 10\%$  from mean period period changed every 10 minutes  
 - - - Constant period test (2 00 sec.)  
 Test time = 40 hours

FIG. 46a - EFFECT OF FREQUENCY OF PERIOD VARIATIONS  
 WATTS (32) 1954

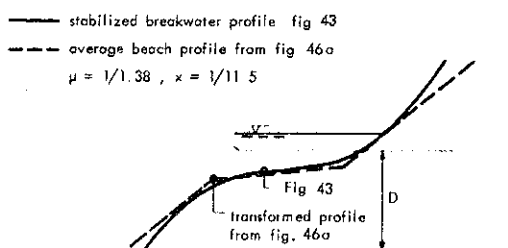


FIG. 46b - BREAKWATER PROFILE (FIG 43) AND TRANSFORMED STEP  
 PROFILE FROM FIG 46a.

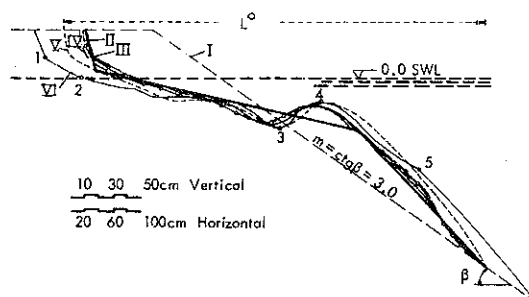


FIG. 47a - MODIFIED DAM PROFILE FROM FIG. 44 USED IN FIG. 47b.

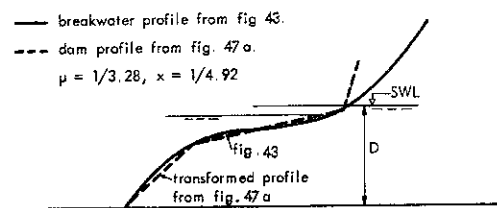


FIG. 47b - BREAKWATER PROFILE (FIG 43) AND TRANSFORMED MODIFIED  
 DAM PROFILE (FIG. 47a)

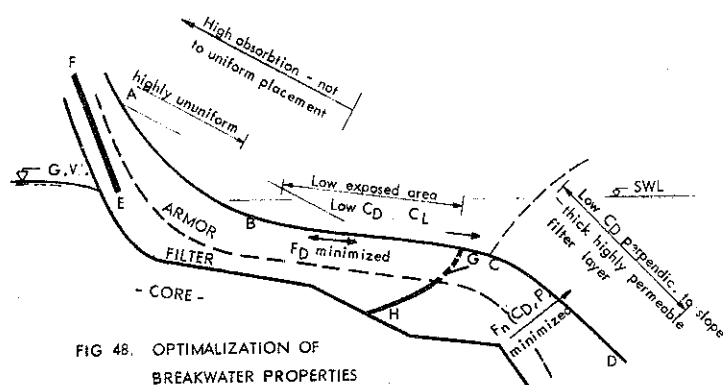


FIG 48. OPTIMIZATION OF  
BREAKWATER PROPERTIES

The false beach, BC, evolves a new breaking point at C which reduces run up (plunging waves and out of phase damping ( $r_d/T/2$ )).

The impervious layer, FE, prevents inflow above point E which reduces the build up of hydrostatic pressure in the mound. The impermeable layer, GH, prevents backwash-outflow to be concentrated at the breaking point, where the external forces are maximized.

The steep slope, CD, makes the backwash-incipient breaker interaction less violent and further separates backwash from the retreating velocity field in the toe of the breaking wave.

The breakwater slope is divided into three zones, each with its characteristic block-properties. This results in more evenly exposed structure which increases safety against failure. In all cases, however, some flexible interlocking effects is very significant.

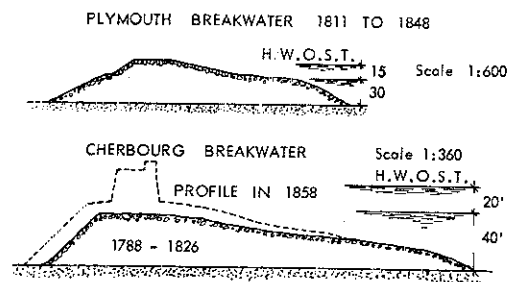


FIG 49. ANCIENT BREAKWATERS AT PLYMOUTH AND  
AT CHERBOURG

PUBLICATIONS AND REPORTS  
BY STAFF MEMBERS OF  
THE DIVISION OF PORTS AND OCEAN ENGINEERING

1970 - 1974

Copies of all published material since 1970 may be ordered by writing "The PUC-Secretary", The Division of Ports and Ocean Engineering, The Norwegian Institute of Technology, 7034 Trondheim, Norway. Inquires on books will be referred to bookstores. For other publications a nominal fee will be charged corresponding to actual printing and handling costs, which, upon request, will be estimated in advance of purchase.

1970

- Faltinsen, O., N. Salvesen, E.O. Tuck,  
"Ship Motions and sea loads", Trans. SNAME, Vol 78,  
1970
- "Predictions of wave-induced motions and loads for  
catamarans", co-author with N. Nordenstrøm and  
B. Pedersen. Offshore Technology Conference,  
Houston 1971
- Houmb, O.G., "Probabilistic and Statistical Evaluation of wave  
Data as an Aid for the Design of Maritime Structures".  
Co-author G. Viggosson, INTEROCEAN Düsseldorf, 1970
- Bruun, P., "New Concept for the Development of Ports", co-author  
H. Loe. Schiff und Hafen, Heft 11, 1970, pp 1045-1049
- Discussion on "Damage Function of Rubble Mound Break-  
waters", ASCE WW2, 1970, pp 559-667

"The Mechanics of Dune Growth by Sand Fences",  
co-author With M. Manohar, The Dock and Harbor  
Authority, vol. LI, No. 600, pp 243-252

1971

- Bratteland, E. "Stability Tests on a Rubble Mound Breakwater Head  
in Regular and Irregular Waves. Sørvar Fishing Port,  
Norway", Co-author A. Tørum. 1st Conf. on Port and  
Ocean Engineering under Arctic Conditions, Vol 1,  
pp 360-380, Trondheim 1971
- Faltinsen, O. "Interaction between soundwaves propagating in the  
same direction", Co-author S. Tjøtta. Proceedings  
from B.A.S. specialist meeting on Nonlinear Underwater  
Acoustics, University of Birmingham, 1971
- Straumsnes, A. "Piling up of Ice on Sea-shores and Coastal Structures"  
Co-author with P. Bruun, IAHR, Ice Symposium,  
Reykjavik, Iceland
- Bruun, P. "Use of Volcanoes for Determination of Littoral Drift",  
co-author G. Viggoson, Proceedings of the 12th Inter-  
national Conference on Coastal Engineering, Washington  
D.C., Sept. 13-18, 1970. (Also published in SURTSEY  
RESEARCH PROGRESS REPORT 1970)

"The future Port and Sedimentation Problems", Schiff  
und Hafen, Heft 2, pp 85-93

"Samvirke mellom is og kystkonstruksjoner"

"Bølgehydraulikk på Rausmoloer"

Korte utgaver av papers presentert ved The First Inter-  
national Conference on Port and Ocean Engineering under  
Arctic Conditions, Trondheim, Aug. 1971, offentliggjort  
i BYGG, nr. 10, Des. 1971.

Medforfattere: A. Straumsnes og P. Johannesson, Papers  
i full format publisert i Proceeding of the first POAC-  
conference, 1972

- Brunvoll, N., "Natural Depths along shores in the North Sea and Adjacent Seas", co-author with H. Loe, Proc. 1st Interna. Conference on Port and Ocean Engineering
- Faltinsen, O., "Wave Forces on a restrained ship in head-sea waves", Proceedings from the Ninth Symposium on Naval Hydrodynamics, Paris, 1972
- Houmb, O.G., "On the Duration of Storms in the North Sea", 1st Conference on Port and Ocean Engineering under Arctic Conditions, Vol. 1 pp 423-439, Trondheim 1971
- Johannesson, P., "Hydraulic Performance of Rubble Mound Breakwaters. Reasons for Failure", Co-author P. Bruun, Proc. 1st Internat Conference on Port and Ocean Engineering under Arctic Conditions, Trondheim, 1971
- "The Interaction between Ice and Coastal Structures", Co-author with P. Bruun, Proc. 1st. International Conference on Port and Ocean Engineering under Arctic Conditions, Trondheim 1971
- Loe, H., "Natural Depths along Shores in the North Sea and Adjacent Seas", Co-author N. Brunvoll, Proc 1st Internat. Conference on Port and Ocean Engineering under Arctic Conditions, Trondheim 1971
- Rye, H., "Long Periodic Oscillations at the Port of Sørvar, the Lopp Sea, Norway", Co-author with G. Viggosson, Proc. 1st Internat. Conference on Port and Ocean Engineering under Arctic Conditions, Trondheim, 1971
- Viggosson, G., "Probability and Statistical Evaluation of Wave Data as an Aid for the Design of Maritime Structures" Co-author with O.G. Houmb, INTEROCEAN, Düsseldorf, 1970

"Long Periodic Oscillations at the Port of Sørvær, The Lopp Sea, Norway", Co-author H. Rye, Proc. 1st Internat Conference on Port and Ocean Engineering under Arctic Conditions, Trondheim, 1971

Vollen, Ø., "Sand Waves on the Bottom of the Sea, with special reference to Conditions in the North Sea", co-author with P. Bruun, Schiff und Hafen, Heft 3, 1972

Bruun, P., "The Interaction between Ice and Coastal Structures". Co-author: Palmi Johannesson. Proceedings of the First International Conference on Port and Ocean Engineering under Arctic Conditions, Technical University of Norway, Trondheim, pp 683-712

"Long-Period Waves in an Icelandic Fiord", co-author with Main Author: Dr. R. Dorrøstein, Nederlandske Meteorologiske Institutt. Proceedings of the First International Conference on Port and Ocean Engineering under Arctic Conditions, Technical University of Norway Trondheim, pp 455-488

"Comparison between Spray and Splash at some typical permeable Coastal Structures and the Influence of Ice Floes deposited on these Structures on Spray and Splash Quantities". Co-author: A. Straumsnes. Proceedings of the First International Conference on Port and Ocean Engineering under Arctic Conditions, Technical University of Norway, Trondheim, pp 713-723

Discussion on "Irregular Waves on Rubble Mound Breakwaters", ASCE, WW1, 1972, pp 113-118

Discussion on "Offshore Floating Terminals", ASCE, WW2, pp 281-282

Institute of Harbour and Ocean Engineering Research "Proceedings of the First International Conference on Port and Ocean Engineering under Arctic Conditions", Vol. 1 and 2, 1460 pp. Edited by



Mrs. S. Stabell Wetteland and Dr. P. Bruun. Printed by The Institute. Distribution in Europe: The Division of Port and Ocean Engineering, The Norwegian Institute of Technology, Trondheim. In the rest of the world: The Gulf Publishing Company, P.O. Box 5608, Houston, Texas, 77001, U.S.A.

1973

- Bratteland, E., "Deep Water Moored Semi-Submersible Platform - Theory and Model Tests". Co-authors S. Leivseth, O. Torset. Proceeding 2nd Conf. on Port and Ocean Engineering under Arctic Conditions, Reykjavik 1973
- "Tracer Project Ekofisk. The North Sea". Co-author P. Bruun. Proceedings 2nd Conf. on Port and Ocean Engineering under Arctic Conditions, Reykjavik 1973
- Houmb, O.G., "Long Term Distribution of North Sea Waves", co-author with L. Håland and B. Pedersen, Norw. Maritime Research Vol 1. No. 1, 1973
- Leivseth, S., "Deep Water Moored Semi-Submersible Platform - Theory and Model Tests". Co-author with E. Bratteland and O. Torset. Proceedings 2nd Conf. on Port and Ocean Engineering under Arctic Conditions, Reykjavik 1973
- Rye, H., "Relative Crest Lengths of Sea and Swell", Journal of Physical Oceanography, Vol.3, No.4, pp 492-493
- Torset, O., "Deep Water Moored Semi-Submersible Platform - Theory and Model Tests". Co-author with E. Bratteland and S. Leivseth. Proceedings 2nd Conf. on Port and Ocean Engineering under Arctic Conditions, Reykjavik 1973
- Bruun, P., "Port Engineering", The Gulf Publishing Company, Houston, Texas, 440 pp
- "The History and Philosophy of Coastal Protection" Proceedings of the 13th Coastal Engineering Conference, Vancouver, B.C., pp 33-74

Paper submitted to the XXIIIrd International Navigation Congress, Ottawa under SII S2 "Means of controlling littoral drift to protect beaches, dunes estuaries and harbour", pp 149-187

1974

Bratteland, E., "Wave Action and Ship Movements in Ports". Proceedings 6th International Harbour Congress, Antwerpen 12-18 May, 1974

Faltinsen, O., "Motions of Large Structures in Waves at Zero Froude Number". Co-author F.C. Michelsen. Proceeding from The International Symposium on The Dynamics of Marine Vehicles and Structures in Waves, University College London, 1974

"A Numerical Investigation of the Ogilvie-Tuck Formulas for Added Mass and Damping Coefficients", Journal of Ship Research, June 1974

"Liquid Slosh in LNG Carriers". Co-author with H.N. Abramson, R.L. Bass and H.A. Olsen, Symposium of Naval Hydrodynamics, Boston, June 1974

"A nonlinear Theory of Sloshing in Rectangular Tanks", Journal of Ship Research, December 1974

Gjertveit, E., "Numerical Calculations of Longperiodic Oscillations at two Norwegian Harbours". Proc. of the 2nd Internat. Conference on Port and Ocean Engineering, Reykjavik 1973

Houmb, O.G., "Analysis of Wave Data from the Norwegian Continental Shelf". Co-author H. Rye. Proceedings 2nd Conf. on Port and Ocean Engineering under Arctic Conditions. Reykjavik 1973

"Numerical Simulation of Currents Recorded in a Norwegian Fiord". Co-author with P. Bruun and H. Rye. Proceedings 2nd Conf. on Port and Ocean Engineering under Arctic Conditions, Reykjavik 1973

"A Norwegian Wave Climate Study". Co-authors B. Pedersen and P. Steinbakke, Waves'74, New Orleans 1974

"Some Experience Gained from Analyses of Visual and Instrumental Wave Data from the Norwegian Continental Shelf". Schiff und Hafen Oct., 1974

"Wave Research at the Norwegian Institute of Technology". Co-author with P. Bruun and J. Strømme. Northern Offshore, March 1974

Torset, O., "Platforms for Conditions in the North Sea", co-author with P. Bruun, Northern Offshore, No. 8, 1974

Bruun, P., "Wave Research at the Norwegian Institute of Technology" Northern Offshore, March Issue. Co-authors O.G. Houmb and J. Strømme

"Platforms for Conditions in the North Sea", Northern Offshore, No. 8, 1974, co-author O. Torset

"Bypassing Sediment - Plants and Arrangements", The Dock and Harbour Authority, London, Vol. LV, No. 645

"The Wave Pump", Proc. of the 2nd. Internat. Conference on Port and Ocean Engineering under Arctic Conditions, Reykjavik, Iceland, 1973. Co-author G. Viggosson

"Littoral Drift on the Icelandic South Coast", Proc. of 2nd. Internat. Conference on Port and Ocean Engineering under Arctic Conditions, Reykjavik, Iceland, 1973